

See discussions, stats, and author profiles for this publication at: <https://www.researchgate.net/publication/259650223>

# Small Molecule Disruptors of the Glucokinase-Glucokinase Regulatory Protein Interaction: 2. Leveraging Structure-Based Drug Design to Identify Analogue... Pharmacokinet...

ARTICLE *in* JOURNAL OF MEDICINAL CHEMISTRY · JANUARY 2014

Impact Factor: 5.45 · DOI: 10.1021/jm4016747 · Source: PubMed

---

CITATIONS

13

---

READS

35

28 AUTHORS, INCLUDING:



Kate S Ashton

Amgen

24 PUBLICATIONS 482 CITATIONS

[SEE PROFILE](#)



Nuria Tamayo

Amgen

38 PUBLICATIONS 1,037 CITATIONS

[SEE PROFILE](#)



Gwyneth Van

Amgen

51 PUBLICATIONS 11,796 CITATIONS

[SEE PROFILE](#)



Kevin Yang

Amgen

14 PUBLICATIONS 218 CITATIONS

[SEE PROFILE](#)

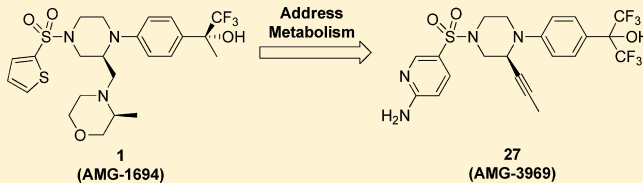
## Small Molecule Disruptors of the Glucokinase–Glucokinase Regulatory Protein Interaction: 2. Leveraging Structure-Based Drug Design to Identify Analogues with Improved Pharmacokinetic Profiles

David J. St. Jean, Jr.,<sup>\*,†</sup> Kate S. Ashton,<sup>†</sup> Michael D. Bartberger,<sup>‡</sup> Jie Chen,<sup>||</sup> Samer Chmait,<sup>‡</sup> Rod Cupples,<sup>§</sup> Elizabeth Galbreath,<sup>†</sup> Joan Helmering,<sup>§</sup> Fang-Tsao Hong,<sup>†</sup> Steven R. Jordan,<sup>‡</sup> Longbin Liu,<sup>†</sup> Roxanne K. Kunz,<sup>†</sup> Klaus Michelsen,<sup>‡</sup> Nobuko Nishimura,<sup>†</sup> Lewis D. Pennington,<sup>†</sup> Steve F. Poon,<sup>†</sup> Darren Reid,<sup>#</sup> Glenn Sivits,<sup>§</sup> Markian M. Stec,<sup>†</sup> Seifu Tadesse,<sup>†</sup> Nuria Tamayo,<sup>†</sup> Gwyneth Van,<sup>†</sup> Kevin C. Yang,<sup>†</sup> Jiandong Zhang,<sup>‡,†</sup> Mark H. Norman,<sup>†</sup> Christopher Fotsch,<sup>†</sup> David J. Lloyd,<sup>§</sup> and Clarence Hale<sup>§</sup>

<sup>†</sup>Department of Therapeutic Discovery—Medicinal Chemistry, <sup>‡</sup>Department of Therapeutic Discovery—Molecular Structure and Characterization, <sup>§</sup>Department of Metabolic Disorders, <sup>||</sup>Department of Pharmacokinetics and Drug Metabolism, <sup>#</sup>Department of Pathology, <sup>#</sup>Department of Pharmaceutics Amgen, Inc., One Amgen Center Drive, Thousand Oaks, California, 91320 and 360 Binney Street, Cambridge, Massachusetts, 02142, United States

### S Supporting Information

**ABSTRACT:** In the previous report, we described the discovery and optimization of novel small molecule disruptors of the GK-GKRP interaction culminating in the identification of **1** (AMG-1694). Although this analogue possessed excellent *in vitro* potency and was a useful tool compound in initial proof-of-concept experiments, high metabolic turnover limited its advancement. Guided by a combination of metabolite identification and structure-based design, we have successfully discovered a potent and metabolically stable GK-GKRP disruptor (**27**, AMG-3969). When administered to *db/db* mice, this compound demonstrated a robust pharmacodynamic response (GK translocation) as well as statistically significant dose-dependent reductions in fed blood glucose levels.



### INTRODUCTION

Small molecule-mediated reduction of blood glucose by allosteric activation of glucokinase (GK) is a well validated pathway.<sup>1–4</sup> Unfortunately, some glucokinase activators (GKAs) have also been linked to a number of undesirable side effects (e.g., hypoglycemia), which have limited their therapeutic potential.<sup>1,5</sup> In an effort to avoid the hypoglycemia observed with GKAs, we focused on identifying compounds that disrupt the glucokinase–glucokinase regulatory protein (GK-GKRP) interaction. By targeting this pathway, the kinetic parameters (i.e.,  $S_{0.5}$  and  $V_{max}$ ) of GK would remain unchanged, which could potentially mitigate the hypoglycemia associated with overactivation.<sup>6</sup> Additionally, because GKRP is predominantly expressed in liver hepatocytes, GK-GKRP modulation would potentially avoid the insulin-mediated reduction in glucose seen with certain GKAs.<sup>7</sup>

In the preceding report, we described the discovery of a novel proof-of-concept tool molecule **1** (AMG-1694).<sup>8</sup> Although this molecule was the first example of a potent GK-GKRP disruptor to demonstrate *in vivo* activity in a rodent model of diabetes,<sup>9</sup> **1** displayed a number of unfavorable characteristics. First, methyl morpholine **1** was extensively metabolized in rats. The formation of a large number of

metabolites complicated the interpretation of subsequent rat toxicology studies involving analogue **1**. Along with the poor rat pharmacokinetic (PK) profile, this molecule also exhibited low exposure in mice. At a 100 mg/kg dose in C57BL/6 mice, the maximum unbound concentration of **1** was significantly less ( $\approx$  50-fold) than the cellular EC<sub>50</sub> value.<sup>10</sup> The combination of poor potency and low exposure of **1** made it difficult to explore small molecule-mediated GK-GKRP disruption in mouse models of diabetes (e.g., *db/db* mice). In addition to the poor rodent PK profiles, this compound was rapidly metabolized in the presence of human liver microsomes ( $CL_{int} = 353 \mu\text{L}/\text{min}/\text{mg}$ ). Given the liabilities of **1**, our focus turned toward the identification of analogues with improved metabolic profiles across species while maintaining or improving biochemical and cellular activity.

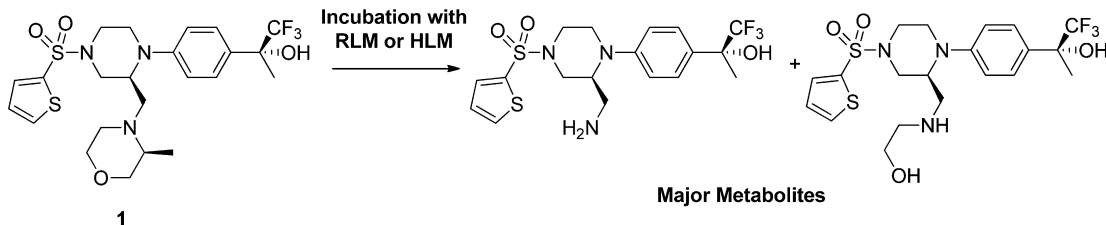
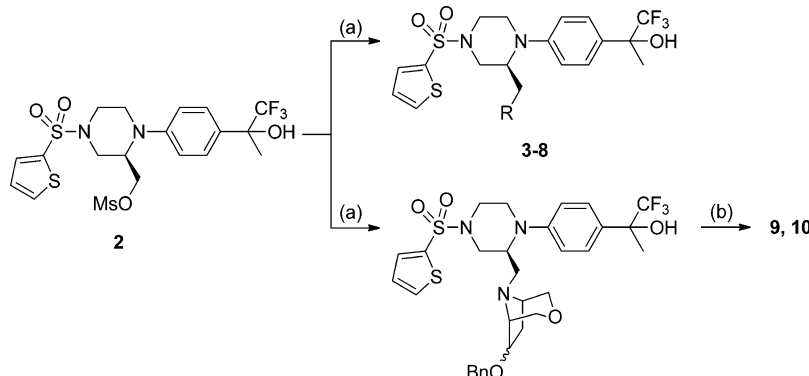
### RESULTS AND DISCUSSION

To address the poor metabolic profile of **1**, metabolite identification studies were performed using both rat and

Received: October 28, 2013

Published: January 9, 2014



**Scheme 1.** In Vitro Metabolism of 1**Scheme 2.** Synthesis of Analogues with Methyl Morpholine Replacements (See Table 1)<sup>a</sup>

<sup>a</sup>Reagents and conditions: (a) secondary amine,  $K_2CO_3$ , MeCN, 140 °C; (b)  $BCl_3$ ,  $CH_2Cl_2$ , 0 °C.

human liver microsomes (RLM/HLM). These experiments revealed that cleavage of the morpholine ring was the primary route of oxidative metabolism (Scheme 1). With a goal to improve the in vitro/in vivo PK profile, we initially sought to replace the metabolically liable methyl morpholine with groups that maintained the overall steric footprint and hydrogen bond acceptor features of 1. To that end, the syntheses of these analogues were straightforward (Scheme 2). Starting from known mesylate 2,<sup>11</sup>  $S_N2$  displacement with a variety of secondary amines provided the desired analogues. The synthesis of the hydroxylated bridged morpholine derivatives (9 and 10) required an additional manipulation ( $BCl_3$ ) to remove a benzyl protecting group installed prior to the amine coupling.

The GKRP activities were evaluated using both a biochemical and cellular assay. The AlphaScreen was a binding assay that measured the ability of a small molecule to disrupt the GK-GKRP interaction.<sup>8</sup> For our primary cellular assay, nuclear to cytoplasmic GK translocation in mouse primary hepatocytes was quantified using an Operetta platform.<sup>9,12</sup> In addition to the primary assays, the in vitro metabolic stabilities were determined using both rat and human liver microsomes.<sup>13</sup> The in vitro profiles of the analogues which contained methyl morpholine replacements are shown in Table 1. To allow for a direct comparison between analogues, 1 was prepared as a mixture of epimers at the tertiary carbinol (3). The 4,4-difluoropiperidine analogue 4 showed significantly weaker potency ( $\approx$  60-fold loss) relative to 3 with no gain in metabolic stability. The sulfone derivative (5) demonstrated an improved LM profile, albeit with a substantial loss in activity. In our previous SAR studies, we demonstrated that the incorporation of a methyl group on the methylene adjacent to the nitrogen atom of the morpholine ring could improve in vitro activity.<sup>8</sup> Application of this strategy to 5 resulted in a modest increase in biochemical activity (6,  $IC_{50} = 0.090 \mu M$ ). Spirocyclic analogue 7 showed an improvement in rat metabolic stability relative to

methyl morpholine 3, but a significant drop in activity was once again observed. Bicyclic morpholine 8 was as potent as analogue 3 but suffered from high microsomal turnover. In an attempt to improve the metabolic stability of 8, hydroxylated analogues 9 and 10 were prepared.<sup>14</sup> Compound 10 showed a significant improvement in LM stability relative to 8, therefore the four stereoisomers of 10 were isolated by chiral SFC (11–14). Unfortunately, despite the promising in vitro activity and improved in vitro stability relative to 3, these analogues displayed poor rat in vivo PK profiles. All four compounds displayed high in vivo clearances (CL), high volumes of distributions ( $V_{ss}$ ), and short mean resonance times (MRT).<sup>15</sup>

Given the poor rat in vivo PK profiles of 11–14, a second metabolite identification study was initiated with bridged morpholine 11 (Scheme 3). Unlike analogue 1, no major metabolites derived from oxidation of the bicyclic morpholine ring were detected. Instead, it was found that metabolism had shifted to the thiophene sulfonamide. Oxidation of the thiophene ring (the molecular structures of these metabolites were not unambiguously assigned) as well as cleavage of the sulfonamide were identified as the major metabolic pathways. Because both the thiophene and the methyl morpholine had been identified as metabolic liabilities, a revision of our overall strategy was necessary. Rather than attempting to block specific sites of metabolism, we chose to revisit the SAR of our initial HTS hit (15, Table 3).<sup>9</sup> By optimizing the sulfonamide present in 15, we hoped to identify a metabolically stable scaffold for which potency could be optimized. Although this analogue contained a metabolically liable thiophene sulfonamide, the in vitro stability and potency were reasonable starting points given its comparatively simple structure relative to 1. To that end, numerous reports have indicated that lowering lipophilicity (i.e., lower clogP) can have beneficial effects on a compound's metabolic profile.<sup>16–18</sup> Additionally, based on the analysis of the cocrystal structure of 1 bound to hGKRP (Figure 1),<sup>9</sup> we rationalized that a hydrogen bond donor could be incorporated

**Table 1. Potency and Microsomal Turnover for Analogs with Methyl Morpholine Replacements**

Cmpd <sup>a</sup>	R	AS IC <sub>50</sub> (μM) <sup>b</sup>	mGK Translocation EC <sub>50</sub> (μM) <sup>c</sup>	RLM CL <sub>int</sub> (μL/min/mg) <sup>d</sup>	HLM CL <sub>int</sub> (μL/min/mg) <sup>d</sup>
3		0.007	0.82	>399	451
4		0.439	>12.5	349	280
5		0.343	>12.5	50	92
6		0.090	>12.5	93	132
7		0.524	>12.5	120	83
8		0.002	0.239	>399	320
9		0.044	1.69	321	302
10		0.026	1.29	141	125
11 <sup>e</sup>		0.014	1.19	118	128
12 <sup>f</sup>		0.016	4.76	114	135
13 <sup>e</sup>		0.025	1.67	155	99
14 <sup>f</sup>		0.056	>12.5	112	131

<sup>a</sup>All compounds were synthesized as mixtures of stereoisomers at the tertiary carbinol unless otherwise noted. <sup>b</sup>AS = hGK-hGKRP AlphaScreen, data reported as an average ( $n \geq 3$ ). Standard deviations are reported in the Supporting Information. <sup>c</sup>Compounds with activities >12.5 μM,  $n = 1$ . For all others, standard deviations ( $n \geq 3$ ) are reported in the Supporting Information. <sup>d</sup>In vitro microsomal stability measurements were conducted in the presence of NADPH at 37 °C for 30 min at a final compound concentration of 1 μM. <sup>e</sup>(R)-Stereoisomer at the CF<sub>3</sub>-tertiary carbinol. The stereochemistry of the secondary alcohol was tentatively assigned based on the analysis of the cocrystal structure with hGKRP. <sup>f</sup>(S)-Stereoisomer at the tertiary CF<sub>3</sub>-carbinol. The stereochemistry of the secondary alcohol was tentatively assigned based on the analysis of the cocrystal structure with hGKRP.

on the thiophene ring. This portion of the GKRP binding site possesses a pair of backbone carbonyl acceptor groups (Gly181 and Met213), conveniently oriented upward toward the thiophene ring. We postulated that the presence of these acceptors in the protein target would permit the introduction of

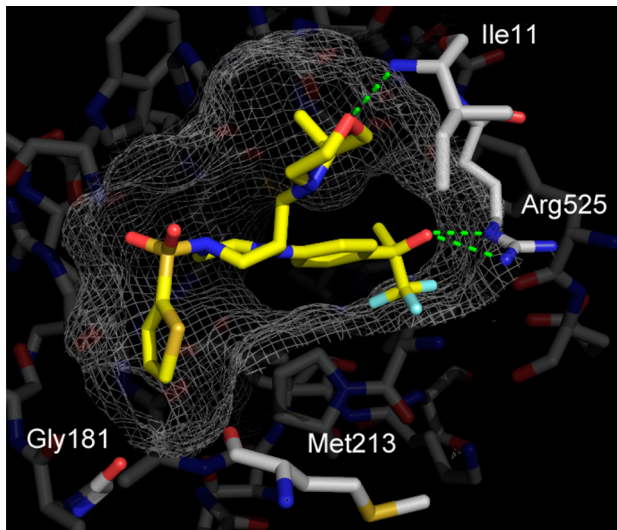
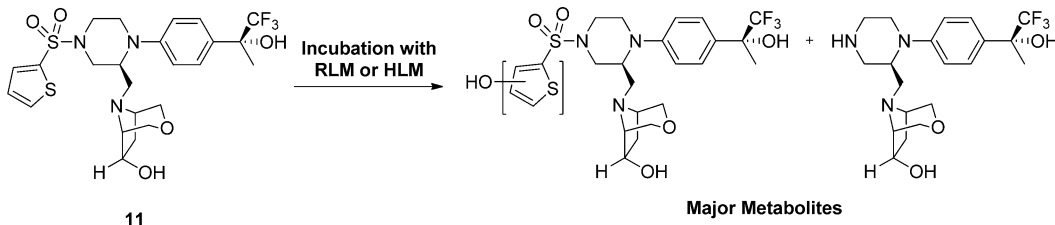
hydrogen bond donor functionality, which would not only engage in electrostatically favorable contacts but would serve to lower lipophilicity as well. Hence, we shifted our focus to the synthesis of compounds that possessed a simplified piperazine core and hydrogen bond donors on the arylsulfonamide functionality.

The syntheses of the analogues which incorporated hydrogen bond donors on the arylsulfonamides are outlined in Scheme 4. To avoid the separation of racemic mixtures, all of the analogues were synthesized with the achiral bis-trifluoromethyl (rather than the methyl-trifluoromethyl) carbinol because these two functionalities were generally equipotent.<sup>9</sup> Starting from 1,1,1,3,3,3-hexafluoro-2-(4-(1-piperazinyl)phenyl)-2-propanol,<sup>9</sup> the formation of thiophenesulfonamide **15** and phenylsulfonamide **16** was straightforward since the sulfonylchlorides were commercially available. The syntheses of the amino-containing analogues required two steps. Aminothiophene analogue **17** was synthesized via a Pd-catalyzed cross-coupling of the 5-bromosulfonamide intermediate with benzophenone imine followed by acidic hydrolysis of the intermediate imine. For analogues **18–21**, sulfonamide formations were accomplished utilizing a nitro-substituted sulfonylchloride followed by reduction of the nitro group using 10% palladium on carbon. The aminopyridine and aminopyrimidine analogues (**22–24**) were synthesized using the corresponding chloro-substituted sulfonyl chlorides followed by aminolysis of the heterocyclic chloride intermediates with concentrated ammonium hydroxide.

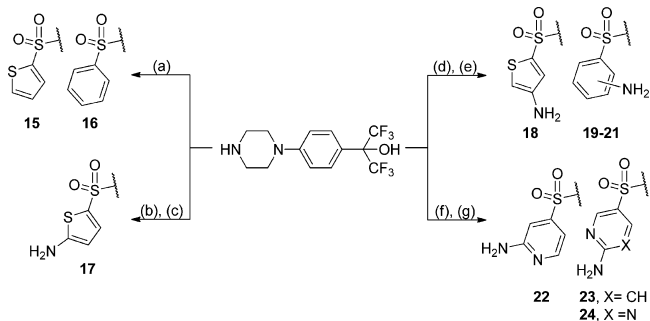
The SAR and clogPs of analogues containing functionalized sulfonamides are shown in Table 2. Both the 5- and 4-aminothiophene derivatives (**17** and **18**) exhibited modest increases in biochemical activity albeit with no improvement in metabolic stability relative to **15**. Replacing the aminothiophene present in these analogues with an aniline resulted in equipotent compounds (**19–21**). Although the potencies were similar, the 3- and 4-amino substituted analogues (**20** and **21**) showed encouraging improvements in rat metabolic stability relative to the unsubstituted parent compound **16**. To further reduce the clogP, additional nitrogen atoms were incorporated into both **20** and **21**. Although aminopyridine **22** displayed a significant loss of activity relative to **20**, the regiosomeric analogue **23** showed a roughly 6-fold increase in biochemical potency relative to **21** with no detectable oxidative metabolism. Aminopyrimidine **24** also exhibited excellent in vitro stability although the potency was slightly lower relative to analogue **23**. Analysis of the X-ray cocrystal structure of **23** bound to hGKRP (Figure 2a) confirmed that this analogue formed two new hydrogen bonding interactions with the backbone carbonyls of Gly181 and Met213. Given the biochemical potency and excellent metabolic stability, this analogue was progressed into a rat in vivo PK study. Relative to **15**,<sup>8</sup> aminopyridine **23** represented a significant improvement in essentially all measurable PK parameters (CL = 0.12 L/h/kg, V<sub>ss</sub> = 1.41 L/kg, MRT = 8.4 h, %F = 71). Despite the excellent rat PK profile, **23** displayed no measurable activity in our cellular assay (EC<sub>50</sub> = >12.5 μM). Nevertheless, we believed that this analogue provided a metabolically stable scaffold from which potency could be optimized.

We have previously reported the existence of a small, hydrophobic subpocket located near Ile11 of the GKRP ligand binding site.<sup>8</sup> Furthermore, we have also shown that occupying this pocket with small alkyl groups can lead to increases in activity. From the analysis of the X-ray cocrystal structures of

Scheme 3. In Vitro Metabolism of 11



**Figure 1.** Compound 1 (yellow) bound to hGKRP. Key residues are highlighted in white, and hydrogen bonding interactions are represented by green dashed lines.

Scheme 4. Synthesis of Sulfonamide Derivatives<sup>a</sup>

<sup>a</sup>Reagents and conditions: (a) 2-thiophenesulfonyl chloride or benzenesulfonyl chloride, NEt<sub>3</sub>, CH<sub>2</sub>Cl<sub>2</sub>, rt; (b) 5-bromo-2-thiophenesulfonyl chloride, NEt<sub>3</sub>, CH<sub>2</sub>Cl<sub>2</sub>, rt; (c) benzophenone imine, t-BuONa, Pd<sub>2</sub>dba<sub>3</sub>, BINAP, toluene, 80 °C then 5 M HCl/THF, rt; (d) 4-nitro-2-thiophenesulfonyl chloride or nitrobenzenesulfonyl chloride, NEt<sub>3</sub>, CH<sub>2</sub>Cl<sub>2</sub>, rt; (e) 10% Pd/C, H<sub>2</sub> (1 atm) EtOH, rt; (f) 6-chloro-3-pyridinesulfonyl chloride, 2-chloro-4-pyridinesulfonyl chloride, or 2-chloro-5-pyrimidinesulfonyl chloride, NEt<sub>3</sub>, CH<sub>2</sub>Cl<sub>2</sub>, rt; (g) NH<sub>4</sub>OH, EtOH, rt or 120 °C.

23 and 1 bound to hGKRP (Figure 2b), we rationalized that a substituted alkyne could replace the metabolically liable methyl morpholine present in 1. It was proposed that this small binding pocket, occupied by the methyl group of 1, could potentially be accessed by a propynyl substituent (i.e.,  $\text{---}\equiv\text{---}$ ). The linear trajectory of the alkyne function would serve to present the terminal methyl group in nearly perfect overlap with the methyl group of 1. This would not only significantly

**Table 2. SAR and cLogPs of Analogue Containing Hydrogen Bond Donating Sulfonamides**

Cmpd	Ar	AS IC <sub>50</sub> ( $\mu\text{M}$ ) <sup>a</sup>	RLM CL <sub>int</sub> ( $\mu\text{L}/\text{min}/\text{mg}$ ) <sup>b</sup>	cLogP <sup>c</sup>
15		1.42	150	3.60
16		1.01	94	3.88
17		0.252	128	2.89
18		0.324	90	2.89
19		0.445	237	3.90
20		0.645	59	3.16
21		0.484	49	3.16
22		8.63	27	2.28
23		0.087	<14	2.28
24		0.316	<14	1.50

<sup>a</sup>AS = hGK-hGKRP AlphaScreen, data reported as an average ( $n \geq 3$ ). Standard deviations are reported in the Supporting Information. All compounds demonstrated cellular EC<sub>50</sub> values of >12.5  $\mu\text{M}$ . <sup>b</sup>In vitro microsomal stability measurements were conducted in the presence of NADPH at 37 °C for 30 min at a final compound concentration of 1  $\mu\text{M}$ . <sup>c</sup>cLogP values were calculated using the PCModels software, version 4.9.2, from Daylight, which is developed and supported by BioByte, Inc., Claremont, CA.

reduce the molecular weight but also lower the number of aliphatic C—H bonds, which could minimize the metabolic liability. Furthermore, the minimal steric bulk of the narrow propynyl substituent would allow a solvating water molecule

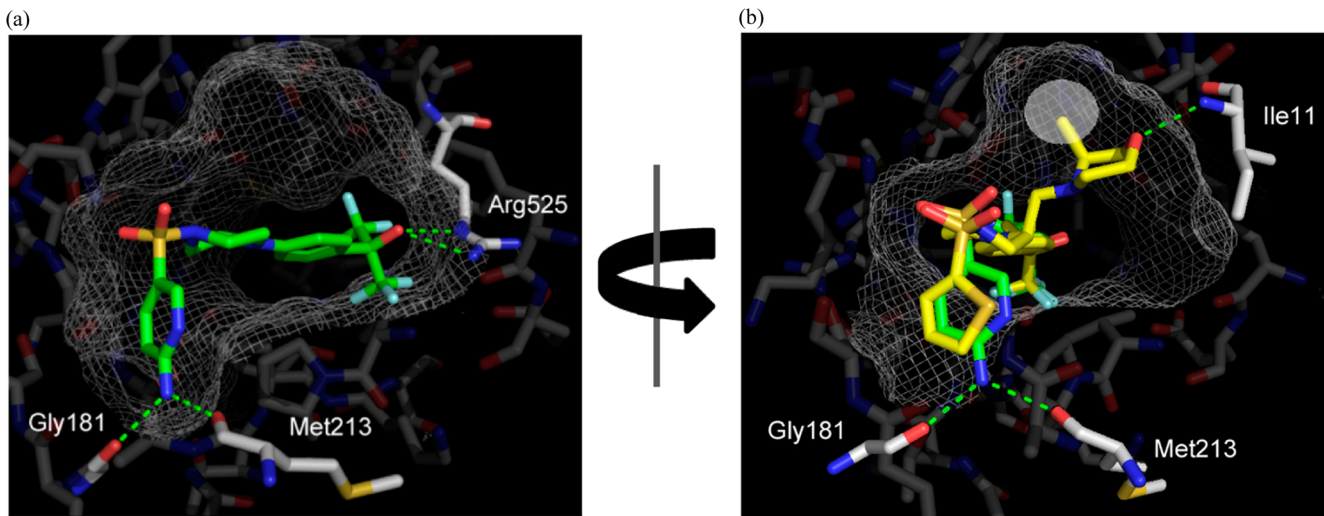
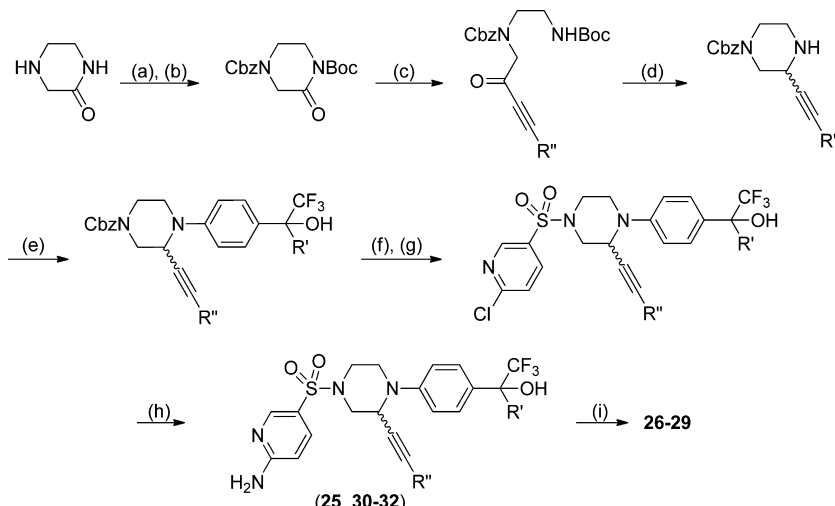


**Figure 2.** (a) Analogue **23** (green) bound to hGKRP. Key residues are highlighted in white, and the hydrogen bonding interactions are represented as green dashed lines. (b) Overlay of compounds **23** (green) and **1** (yellow) bound to hGKRP (rotated relative to (a)). The hydrophobic subpocket is highlighted by a white oval.

**Scheme 5. Synthesis of Alkynyl-Substituted Piperazines (See Table 3)<sup>a</sup>**



<sup>a</sup>Reagents and conditions: (a) benzyl chloroformate,  $\text{Na}_2\text{CO}_3$ , dioxane/water, rt; (b)  $(\text{Boc})_2\text{O}$ ,  $\text{NEt}_3$ , DMAP,  $\text{CH}_2\text{Cl}_2$ , rt; (c) alkynyl Grignard reagents, THF, 0 °C; (d) TFA,  $\text{CH}_2\text{Cl}_2$  then  $\text{NaBH}(\text{OAc})_3$ , rt; (e) 2-(4-bromophenyl)-1,1,3,3-hexafluoro-2-propanol or 2-(4-bromophenyl)-1,1,1-trifluoropropan-2-ol, RuPhos first generation precatalyst, RuPhos,  $\text{NaOt-Bu}$ , toluene, 100 °C; (f) TfOH, TFA, rt; (g) 6-chloropyridine-3-sulfonyl chloride,  $\text{NEt}_3$ ,  $\text{CH}_2\text{Cl}_2$ , rt; (h)  $\text{NH}_4\text{OH}/\text{EtOH}$ , 110–120 °C; (i) chiral SFC.

(rather than the morpholine oxygen atom in **1**) to satisfy the backbone donor NH of Ile11.<sup>19</sup> Access to this methyl-accommodating subpocket directly from the piperazine core would require an axial-like disposition of the linear substituent. Gratifyingly, this orientation was predicted from quantum mechanical calculations to be the lowest-energy conformation in the unbound state.<sup>20</sup>

The syntheses of these alkynyl-substituted derivatives are shown in Scheme 5. Starting from the commercially available 2-piperazinone, two sequential protections (Cbz followed by Boc) proceeded in high yield. A variety of alkynyl Grignard reagents were added into the imide carbonyl to provide the corresponding ketone intermediates. Trifluoroacetic acid-mediated removal of the Boc group, followed by in situ reduction of the resultant imine, provided the racemic piperazines. *N*-Arylation,<sup>21</sup> removal of the Cbz protecting group, and sulfonamide formation using 6-chloropyridine-3-

sulfonyl chloride<sup>22</sup> delivered the penultimate intermediates. Formation of the aminopyridine functionality was accomplished by treating the chloropyridines with ammonium hydroxide in ethanol. For the most promising analogues, the individual stereoisomers were isolated using chiral SFC.

The GKR activities and the metabolic stabilities of the alkynyl-substituted piperazine analogues are shown in Table 3. Incorporation of the methyl substituted alkyne (**25**) had a dramatic effect on the biochemical potency when compared to the unsubstituted piperazine (**23**). More importantly, the cellular potency of **25** was significantly improved without a deleterious drop in metabolic stability. The more active enantiomer, **27** (AMG-3969), exhibited both potent cellular activity ( $\text{EC}_{50} = 0.202 \mu\text{M}$ ) and excellent metabolic stability when exposed to rat/human liver microsomes (42 and <14  $\mu\text{L}/\text{min}/\text{mg}$ , respectively). Analysis of the cocrystal structure of **27** bound to hGKRP (Figure 3) confirmed that the terminal

Table 3. Potency and Microsomal Turnover of Alkynyl-Substituted Piperazines

Cmpd	R	R'	AS IC <sub>50</sub> (μM) <sup>a</sup>	mGK Translocation EC <sub>50</sub> (μM) <sup>b</sup>	RLM CL <sub>int</sub> (μL/min/mg) <sup>c</sup>	HLM CL <sub>int</sub> (μL/min/mg) <sup>c</sup>
23	H	CF <sub>3</sub>	0.087	>12.5	<14	<14
25		CF <sub>3</sub>	0.006	0.455	72	<14
26		CF <sub>3</sub>	0.484	>12.5	119	<14
27 (AMG-3969)		CF <sub>3</sub>	0.004	0.202	42	<14
28		Me-(S)	0.006	0.227	71	<14
29		Me-(R)	0.009	0.120	39	<14
30		CF <sub>3</sub>	0.056	2.93	109	<14
31		CF <sub>3</sub>	0.779	>12.5	61	52
32		CF <sub>3</sub>	1.43	>12.5	90	<14

<sup>a</sup>AS = hGK-hGKRP AlphaScreen, data reported as an average ( $n \geq 3$ ). Standard deviations are reported in the Supporting Information.

<sup>b</sup>Compounds with activities >12.5 μM,  $n = 1$ . For all others, standard deviations ( $n \geq 3$ ) are reported in the Supporting Information. <sup>c</sup>In vitro microsomal stability measurements were conducted in the presence of NADPH at 37 °C for 30 min at a final compound concentration of 1 μM.

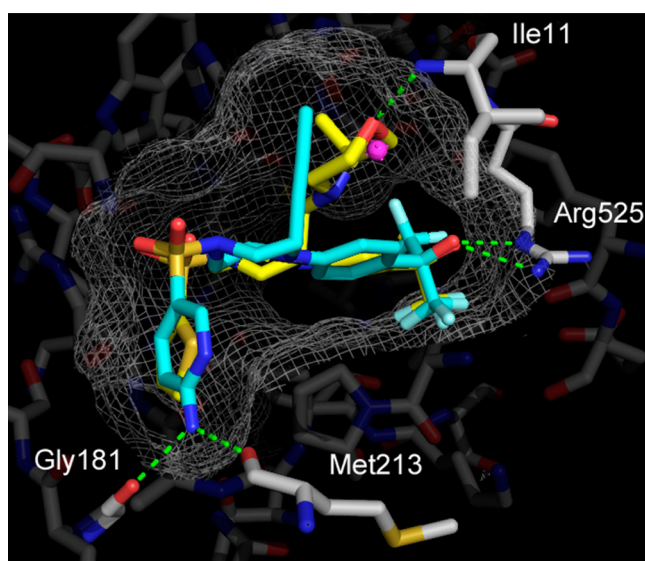


Figure 3. Overlay of analogues 27 (blue, shown with an active site water molecule (pink)) and 1 (yellow) bound to hGKRP. Key protein residues are highlighted in white, while hydrogen bonding interactions are represented as green dashed lines.

methyl group occupied the same hydrophobic pocket as the methyl group on the morpholine ring of 1. Analogs 28 and

29 also showed promising in vitro activities and excellent rat and human in vitro metabolic stabilities. Unfortunately, attempts to further improve activity by incorporating larger hydrophobic groups at the terminal end of the alkyne (i.e., 30–32) did not lead to further improvements in activity.

Given the promising activity and metabolic profiles of 27–29, each of these molecules were progressed into rat in vivo PK studies (Table 4). Compounds 27 and 29 displayed excellent PK profiles when compared to methylmorpholine 1. Both compounds had in vivo clearances significantly less than liver blood flow (10–20%) with excellent bioavailabilities (>75%).

Table 4. In Vivo PK and PPB Data for Compounds 27, 28, 29, and 1

species	compd	CL (L/h/kg) <sup>a</sup>	V <sub>ss</sub> (L/kg) <sup>a</sup>	MRT (h)	%F <sup>b</sup>	f <sub>u</sub> (%) <sup>c</sup>
rat	27	0.75	3.6	6.2	75	1.5
rat	28	1.8	3.7	2.9	57	3.6
rat	29	0.39	1.6	4.6	82	2.7
rat	1	4.1	8.3	4.4	7	3.7
mouse	27	0.11	1.1	9.2	40	1.2
mouse	29	0.18	1.0	5.3	39	2.3

<sup>a</sup>2 mg/kg intravenous dose (100% DMSO). <sup>b</sup>10 mg/kg oral dose (1% Tween 80, 2% HPMC, 97% water, pH = 7.0). <sup>c</sup>Fraction unbound was determined via rapid equilibrium dialysis.

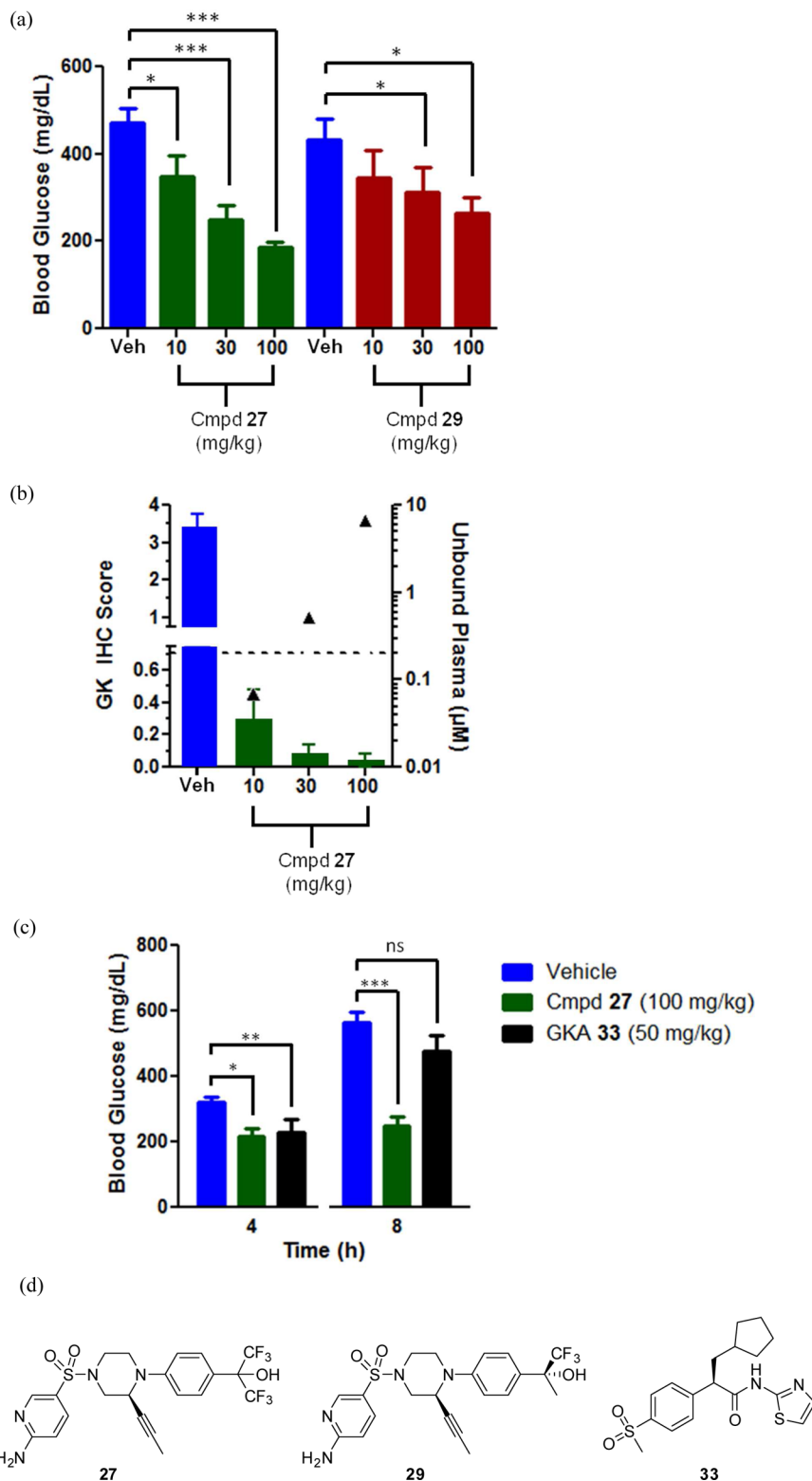


**Figure 4.** (a) Blood glucose measurements 6 h postoral administration of **27** (green bars) and **29** (red bars) (10, 30, 100, mg/kg) to *db/db* mice. The statistical significance of the blood glucose measurements were based on comparison to the individual vehicle (Veh) control groups (blue bars,  $n \geq 6$ , \* =  $p < 0.05$ , \*\*\* =  $p < 0.001$ ). (b) In vivo GK translocation (green bars, left y-axis) and unbound plasma concentrations (black triangles, right y-axis) in *db/db* mice following oral administration of **27** (10, 30, 100 mg/kg, 6 h postdose). The dotted line represents the GK translocation EC<sub>50</sub> value for **27** ( $0.202 \mu\text{M}$ ) in mouse hepatocytes. (c) Blood glucose measurements of *db/db* mice following administration of either **27** (green bars, 100 mg/kg, po) or GKA 33 (black bars, 50 mg/kg, po) at 4 and 8 h postdose. The statistical significance of the blood glucose measurements were determined based on comparison to the individual vehicle (Veh) control groups (blue bars,  $n \geq 7$ , \* =  $p < 0.05$ , \*\* =  $p < 0.01$ , \*\*\* =  $p < 0.001$ , ns = not significant). (d) Molecular structures of **27**, **29**, and **33**.

For compound **28**, the modestly higher microsomal turnover ( $71 \mu\text{L}/\text{min}/\text{mg}$ ) translated to an increase in *in vivo* clearance relative to both **27** and **29**. Both **27** and **29** also demonstrated excellent *in vivo* PK profiles in mice (Table 4). The unbound drug concentrations (10 mg/kg, po) in the mouse PK study approached or exceeded the cellular EC<sub>50</sub> values for both **27** and **29** (concentrations at C<sub>max</sub> were 0.068 and 0.292  $\mu\text{M}$ , respectively). Because the mouse PK profiles allowed for *in vivo* coverage of the *in vitro* EC<sub>50</sub> values, both of these analogues were administered to *db/db* mice to determine the effect of small molecule-mediated GK-GKRP disruption on fed blood glucose levels.

Genetically obese, insulin resistant diabetic *db/db* mice are commonly used to monitor the efficacy of glucose lowering agents.<sup>23</sup> At 6 h postoral administration with either **27** or **29**, a statistically significant dose-dependent reduction in fed blood glucose levels was observed (Figure 4a). Because analogue **27** demonstrated a more robust *in vivo* response when compared to **29**,<sup>24</sup> the livers of the animals treated with compound **27** were examined to determine the extent of the GK translocation via immunohistochemistry (IHC). An IHC score of four represented no pharmacodynamic (PD) response, while a score of zero indicated essentially complete nuclear translocation of GK. As shown in Figure 4b, an IHC score of approximately zero was observed at both the 30 and 100 mg/kg doses of **27**, which corresponded to 47% and 60% reductions in blood glucose, respectively. The exposure from this efficacy experiment also demonstrated a reasonable correlation to the *in vitro* potency. Statistically significant reductions in blood glucose were observed at systemic free drug concentrations near the mouse hepatocytes cellular EC<sub>50</sub> values for both **27** and **29**.<sup>25</sup> In a subsequent experiment, we investigated two additional time points following an oral dose of compound **27** with the purpose of comparing to a known GKA (33) published by Roche (Figure 4c).<sup>26</sup> As shown in Figure 4c, analogue **27** (100 mg/kg) demonstrated significant reductions in blood glucose with robust efficacy (56% reduction) observed at the 8 h time point. Although GKA 33 (50 mg/kg)<sup>26</sup> was efficacious at the early (4 h) time point, no statistically significant reduction in fed blood glucose was observed at 8 h postdose.<sup>27</sup>

## CONCLUSION

By relying heavily on metabolite identification and structure-based drug design, we systematically eliminated a number of metabolic liabilities present in **1**. By replacing both the thiophene and the methyl morpholine functionalities, we successfully identified a potent and metabolically stable GK-GKRP disruptor (**27**). This compound represents the first compound from this class to demonstrate *in vivo* efficacy in a mouse model of diabetes. Furthermore, analogue **27** did not bind to GK itself, hence the robust *in vivo* efficacy observed with this compound was not a result of GK activation.<sup>28</sup> Also, consistent with our initial report, no signs of hypoglycemia were observed in animals (either normal or hyperglycemic) when treated with compound **27**.<sup>9</sup> Hence, the lack of hypoglycemia combined with the significant glucose lowering observed in *db/db* mice provide compelling evidence to support GK-GKRP disruption as a potential treatment for diabetes.

## EXPERIMENTAL SECTION

**A. Biology.** *1. hGK-hGKRP AlphaScreen.* This assay was conducted as previously reported.<sup>9,10</sup>

**2. GK Translocation in Mouse Hepatocytes.** Mouse hepatocytes<sup>29</sup> in maintenance media (Williams E, 10% FBS, 1  $\times$  PSG, 1  $\mu\text{g}/\text{mL}$  insulin, 100 nM dexamethasone) were plated into a 96-well plate (50000 cells/well) and incubated overnight. Cells were washed twice (200  $\mu\text{L}$  of DMEM no glucose/0.2% BSA), then 100  $\mu\text{L}$  of DMEM (no glucose)/0.2% BSA was added and cells were incubated for 3–4 h at 37 °C. Cells were again washed with DMEM (no glucose) only, and test compounds diluted in DMEM (no glucose) were added, incubated for 20 min at 37 °C, followed by addition of 10  $\mu\text{L}$  of 25 mM glucose and further incubated for an additional 40 min at 37 °C. Cells were then fixed (100  $\mu\text{L}$  of 8% formaldehyde/PBS), and the plates were incubated at rt for 15 min, washed twice with 200  $\mu\text{L}$  of PBS, then permeabilized (75  $\mu\text{L}$  of 0.3% Triton X-100/PBS) for 10 min. Following two washes with 200  $\mu\text{L}$  of PBS, 50  $\mu\text{L}$  of blocking solution (Li-Cor) was added and incubated for 1 h at rt. Cells were washed (100  $\mu\text{L}$  of 1% goat serum/0.1% Tween in PBS), incubated with 50  $\mu\text{L}$  of anti-GK antibody diluted 1:125 in 1:1 Li-Cor blocking:wash buffer, incubated at 4 °C overnight, and, after washing, 50  $\mu\text{L}$  of goat antirabbit AlexaFluor 555 diluted 1:100 and 1  $\mu\text{g}/\text{mL}$  of Hoechst 33342 in wash buffer was added to each well and incubated for 1 h at rt. Following washing, 200  $\mu\text{L}$  of PBS was added to each well and imaging was performed using an Operetta system (PerkinElmer).

**3. In Vivo Studies in db/db Mice.** Diabetic *db/db* mice were purchased from Jackson Laboratories at 8–9 weeks of age and cared for in accordance to the *Guide for the Care and Use of Laboratory Animals*, 8th ed. Animals were housed four per cage at an AAALAC, Intl-accredited facility in a ventilated microisolator on corn cob bedding. All research protocols were approved by the Amgen, Inc., Institutional Animal Care and Use Committee. Animals had ad libitum access to pelleted chow and water and were maintained on a 12:12 h light:dark cycle with nestlet enrichment opportunities and acclimatized for 1 week. All animals were determined specific pathogen free. At 8:00 AM, mice were bled via retro-orbital sinus puncture and blood glucose values were determined (AlphaTRAK glucose meter) and used to randomize the animals in which their averages were similar, and only mice with blood glucose ranges between 300 and 500 mg/dL were included. Vehicle (2% hydroxypropyl methylcellulose, 1% Tween 80, pH 2.2 adjusted with MSA), **27**, **29**, or **33** formulations were gavaged at 9:00 AM. Blood glucose was measured at 4, 6, or 8 h post-treatment. At each time point, a 15  $\mu\text{L}$  sample of whole blood was analyzed for drug exposure. SAS version 9.2 on a Linux system was used to perform all statistical analyses by ANCOVA.

For IHC studies, mice were sacrificed following anesthesia, and liver samples were immediately excised (2–3 mm thick and 7–8 mm long, from the right medial and the left lateral lobe), fixed in cold paraformaldehyde for 3 h, and transferred to 70% EtOH prior to processing and embedding in paraffin. Then 5  $\mu\text{m}$  thick sections of paraffin-embedded liver were deparaffinized and hydrated in DI H<sub>2</sub>O. Sections were pretreated with Diva Decloaker (Biocare Medical) in a pressure cooker, blocked with CAS-Block (Invitrogen), and incubated with rabbit anti-GK antibody (Santa Cruz Biotechnologies) at 1:100 for 1 h at rt. Slides were quenched with 3% H<sub>2</sub>O<sub>2</sub>, followed with EnVision + HRP labeled polymer antirabbit (DAKO). Reaction sites were visualized with DAB (DAKO), and slides were counterstained with hematoxylin. Slides were independently evaluated for nuclear GK intensity by two observers without knowledge of treatment group.

**B. Chemistry.** Unless otherwise noted, all reagents were commercially available and used as received. All final compounds possessed purity  $\geq 95\%$  as determined by high performance liquid chromatography (HPLC). The HPLC methods used the following conditions: Zorbax SB-C18 column (50 mm  $\times$  3.0 mm, 3.5  $\mu\text{m}$ ) at 40 °C with a 1.5 mL/min flow rate; solvent A of 0.1% TFA in water, solvent B of 0.1% TFA in MeCN; 0.0–3.0 min, 5–95% B in A; 3.0–3.5 min, 95% B in A; 3.5–3.51 min, 5% B in A. Flow from the UV detector was split (50:50) to the MS detector which was configured with APIES as ionizable source. <sup>1</sup>H NMR spectra were recorded on a 300 or 400 MHz Bruker NMR spectrometer at ambient temperature. Data are reported as follows: chemical shift (ppm,  $\delta$  units) from an internal standard, multiplicity (s = singlet, d = doublet, t = triplet, q = quartet, m = multiplet, and br = broad), coupling constant (Hz), and

integration. All microwave-assisted reactions were performed in sealed reaction vials using a Personal Chemistry Emrys Optimizer microwave synthesizer. Analytical thin-layer chromatography (TLC) was performed using JT Baker silica gel plates precoated with a fluorescent indicator. Silica gel chromatography was performed using either an ISCO Companion or Biotage medium pressure liquid chromatography system.

**1,1,1-Trifluoro-2-(4-((2S)-2-((3S)-3-methyl-4-morpholinyl)methyl)-4-(2-thiophenylsulfonyl)-1-piperazinyl)phenyl)-2-propanol (3).** A 20 mL microwave vial was charged with ((2R)-4-(2-thiophenylsulfonyl)-1-(4-(2,2,2-trifluoro-1-hydroxy-1-methylethyl)-phenyl)-2-piperazinyl)methyl methanesulfonate<sup>11</sup> (0.50 g, 0.95 mmol), (S)-3-methylmorpholine (0.191 g, 1.89 mmol), and 7 mL of MeCN. The vial was sealed and heated in a microwave synthesizer at 125 °C for 1 h. The mixture was allowed to cool to rt and then diluted with 10 mL of EtOAc and filtered. The filtrate was concentrated and purified via silica gel chromatography (0–70% EtOAc in hexanes) to produce the title compound (0.050 g, 0.094 mmol, 10% yield) as a white solid. <sup>1</sup>H NMR (400 MHz, CD<sub>3</sub>OD) δ 7.90 (dd, *J* = 1.2, 5.1 Hz, 1 H), 7.66 (dd, *J* = 1.4, 3.7 Hz, 1 H), 7.46 (d, *J* = 8.8 Hz, 2 H), 7.28 (dd, *J* = 3.8, 5.0 Hz, 1 H), 6.94 (d, *J* = 8.8 Hz, 2 H), 4.12–3.92 (m, 2 H), 3.85–3.40 (m, 6 H), 3.29–3.07 (m, 2 H), 2.87 (d, *J* = 11.7 Hz, 1 H), 2.70–2.45 (m, 2 H), 2.34 (t, *J* = 6.0 Hz, 1 H), 2.19–2.00 (m, 1 H), 1.88 (d, *J* = 12.3 Hz, 1 H), 1.69 (s, 3 H), 1.02 (d, *J* = 6.2 Hz, 3 H). *m/z* (ESI, +ve ion) 534.0 (M + H)<sup>+</sup>.

**2-(4-((2S)-2-((4,4-Difluoro-1-piperidinyl)methyl)-4-(2-thiophenylsulfonyl)-1-piperazinyl)phenyl)-1,1-trifluoro-2-propanol (4).** Following the procedure outlined above for 3, the reaction of 4,4-difluoropiperidine and ((2R)-4-(2-thiophenylsulfonyl)-1-(4-(2,2,2-trifluoro-1-hydroxy-1-methylethyl)phenyl)-2-piperazinyl)methyl methanesulfonate produced the title compound (51% yield). <sup>1</sup>H NMR (400 MHz, CD<sub>3</sub>OD) δ 7.89 (dd, *J* = 1.2, 5.1 Hz, 1 H), 7.66 (dd, *J* = 1.2, 3.7 Hz, 1 H), 7.45 (d, *J* = 8.8 Hz, 2 H), 7.27 (dd, *J* = 3.8, 5.0 Hz, 1 H), 6.93 (d, *J* = 8.8 Hz, 2 H), 4.19–4.01 (m, 1 H), 3.96 (d, *J* = 11.2 Hz, 1 H), 3.79 (d, *J* = 9.4 Hz, 1 H), 3.45–3.24 (m, 2 H), 3.24 (dt, *J* = 3.5, 12.0 Hz, 1 H), 2.78 (dd, *J* = 9.2, 12.9 Hz, 1 H), 2.71–2.55 (m, 3 H), 2.55–2.44 (m, 2 H), 2.38 (dd, *J* = 4.8, 12.8 Hz, 1 H), 1.91–1.74 (m, 4 H), 1.69 (s, 3 H). *m/z* (ESI, +ve ion) 554.2 (M + H)<sup>+</sup>.

**2-(4-((2S)-2-((1,1-Dioxido-4-thiomorpholinyl)methyl)-4-(2-thiophenylsulfonyl)-1-piperazinyl)phenyl)-1,1-trifluoro-2-propanol (5).** Following the procedure outlined above for 3, the reaction of thiomorpholine 1,1-dioxide and ((2R)-4-(2-thiophenylsulfonyl)-1-(4-(2,2,2-trifluoro-1-hydroxy-1-methylethyl)phenyl)-2-piperazinyl)methyl methanesulfonate produced the title compound (12% yield) as an off-white solid. <sup>1</sup>H NMR (400 MHz, CD<sub>3</sub>OD) δ 7.91 (dd, *J* = 1.3, 5.0 Hz, 1 H), 7.68 (dd, *J* = 1.4, 3.7 Hz, 1 H), 7.48 (d, *J* = 8.8 Hz, 2 H), 7.29 (dd, *J* = 3.7, 5.1 Hz, 1 H), 6.98–6.92 (m, 2 H), 4.15 (br. s, 1 H), 3.98 (br d, *J* = 11.2 Hz, 1 H), 3.83 (br d, *J* = 11.3 Hz, 1 H), 3.47 (d, *J* = 12.5 Hz, 1 H), 3.32–3.22 (m, 1 H), 3.09–2.75 (m, 9 H), 2.74–2.50 (m, 3 H), 1.70 (s, 3 H). *m/z* (ESI, +ve ion) 567.8 (M + H)<sup>+</sup>.

**1,1,1-Trifluoro-2-(4-((2S)-2-((3-methyl-1,1-dioxido-4-thiomorpholinyl)methyl)-4-(2-thiophenylsulfonyl)-1-piperazinyl)phenyl)-2-propanol (6).** Following the procedure outlined above for 3, the reaction of 3-methylthiomorpholine 1,1-dioxide<sup>30</sup> and ((2R)-4-(2-thiophenylsulfonyl)-1-(4-(2,2,2-trifluoro-1-hydroxy-1-methylethyl)phenyl)-2-piperazinyl)methyl methanesulfonate produced the title compound (35% yield) as an off-white solid. <sup>1</sup>H NMR (400 MHz, CD<sub>3</sub>OD) δ 7.90 (dd, *J* = 1.2, 5.1 Hz, 1 H), 7.73–7.59 (m, 1 H), 7.55–7.37 (m, 2 H), 7.27 (dd, *J* = 3.7, 4.9 Hz, 1 H), 6.94 (dd, *J* = 2.9, 9.0 Hz, 2 H), 4.14–3.97 (m, 2 H), 3.79 (d, *J* = 11.0 Hz, 1 H), 3.47–3.17 (m, 3 H), 3.11–2.73 (m, 7 H), 2.65–2.37 (m, 3 H), 1.68 (s, 3 H), 1.28–1.21 (m, 3 H). *m/z* (ESI, +ve ion) 581.9 (M + H)<sup>+</sup>.

**1,1,1-Trifluoro-2-(4-((2S)-2-(2-oxa-6-azaspiro[3.3]hept-6-ylmethyl)-4-(2-thiophenylsulfonyl)-1-piperazinyl)phenyl)-2-propanol (7).** Following the procedure outlined above for 3, the reaction of 2-oxa-6-azaspiro[3.3]heptane and ((2R)-4-(2-thiophenylsulfonyl)-1-(4-(2,2,2-trifluoro-1-hydroxy-1-methylethyl)phenyl)-2-piperazinyl)methyl methanesulfonate produced the title compound (32% yield). <sup>1</sup>H NMR (400 MHz, CD<sub>3</sub>OD) δ 7.89 (d, *J* = 5.1 Hz, 1 H), 7.65 (d, *J* = 3.7 Hz, 1 H), 7.47 (d, *J* = 8.8 Hz, 2 H), 7.33–7.21 (m, 1 H), 6.97–6.85 (m, 2 H), 4.69 (br. s, 4 H), 3.90–3.66 (m, 3 H), 3.52–3.38 (m, 3 H), 3.27–

3.11 (m, 1 H), 2.97–2.83 (m, 1 H), 2.66 (dd, *J* = 2.8, 11.4 Hz, 1 H), 2.57 (dt, *J* = 3.8, 11.4 Hz, 1 H), 2.36 (br d, *J* = 12.1 Hz, 1 H), 1.69 (s, 3 H), 1.24–1.19 (m, 1 H), 1.06–0.99 (m, 1 H). *m/z* (ESI, +ve ion) 532.1 (M + H)<sup>+</sup>.

**1,1,1-Trifluoro-2-(4-((2S)-2-(3-oxa-8-azabicyclo[3.2.1]oct-8-ylmethyl)-4-(2-thiophenylsulfonyl)-1-piperazinyl)phenyl)-2-propanol (8).** Following the procedure outlined above for 3, the reaction of 3-oxa-8-azabicyclo[3.2.1]octane and ((2R)-4-(2-thiophenylsulfonyl)-1-(4-(2,2,2-trifluoro-1-hydroxy-1-methylethyl)phenyl)-2-piperazinyl)methyl methanesulfonate produced the title compound (10% yield). <sup>1</sup>H NMR (400 MHz, CDCl<sub>3</sub>) δ 7.64 (dd, *J* = 1.2, 5.1 Hz, 1 H), 7.61–7.55 (m, 1 H), 7.42 (d, *J* = 8.8 Hz, 2 H), 7.17 (dd, *J* = 3.7, 4.9 Hz, 1 H), 6.80 (d, *J* = 8.8 Hz, 2 H), 4.21 (d, *J* = 11.2 Hz, 1 H), 3.95–3.75 (m, 2 H), 3.66–3.53 (m, 2 H), 3.52–3.37 (m, 3 H), 3.20 (dt, *J* = 3.4, 12.0 Hz, 1 H), 3.09–2.99 (m, 1 H), 2.97–2.86 (m, 1 H), 2.71–2.47 (m, 3 H), 2.34 (br s, 1 H), 2.19 (dd, *J* = 3.3, 12.5 Hz, 1 H), 1.89–1.49 (m, 7 H). *m/z* (ESI, +ve ion) 546.0 (M + H)<sup>+</sup>.

**8-((2S)-4-(2-Thiophenylsulfonyl)-1-(4-(2,2,2-trifluoro-1-hydroxy-1-methylethyl)phenyl)-2-piperazinyl)methyl-3-oxa-8-exo-azabicyclo[3.2.1]octan-6-ol (9).** Following the two-step procedure reported for 10, 3-oxa-8-exo-azabicyclo[3.2.1]octan-6-ol hydrochloride<sup>14</sup> delivered the title compound as a white solid (mixture of four isomers, 10% yield over two steps). <sup>1</sup>H NMR (400 MHz, CD<sub>3</sub>OD) δ 7.89 (d, *J* = 5.1 Hz, 1 H), 7.67 (br s, 1 H), 7.44 (dd, *J* = 8.8, 12.5 Hz, 2 H), 7.28 (t, *J* = 4.0 Hz, 1 H), 6.92 (dd, *J* = 6.8, 8.8 Hz, 2 H), 4.64–4.37 (m, 1 H), 4.28–3.72 (m, 3 H), 3.62–2.83 (m, 10 H), 2.70–2.50 (m, 3 H), 2.24–2.03 (m, 1 H), 1.76–1.64 (m, 3 H). *m/z* (ESI, +ve ion) 562.1 (M + H)<sup>+</sup>.

**8-((2S)-4-(2-Thiophenylsulfonyl)-1-(4-(2,2,2-trifluoro-1-hydroxy-1-methylethyl)phenyl)-2-piperazinyl)methyl-3-oxa-8-endo-azabicyclo[3.2.1]octan-6-ol (10).** A 10 mL vial was charged with ((2R)-4-(2-thiophenylsulfonyl)-1-(4-(2,2,2-trifluoro-1-hydroxy-1-methylethyl)phenyl)-2-piperazinyl)methyl methanesulfonate<sup>11</sup> (0.207 g, 0.391 mmol), 6-(benzyloxy)-3-oxa-8-endo-azabicyclo[3.2.1]octane hydrochloride<sup>14</sup> (0.100 g, 0.391 mmol), potassium carbonate (0.162 g, 1.17 mmol), and 3 mL of MeCN. The tube was sealed and heated in a microwave reactor at 150 °C for 1 h. The mixture was allowed to cool to rt and then diluted with 5 mL of EtOAc and filtered. The filtrate was concentrated and purified via silica gel chromatography (0–50% EtOAc in hexanes) to give 2-(4-((2S)-2-((6-(benzyloxy)-3-oxa-8-endo-azabicyclo[3.2.1]oct-8-yl)methyl)-4-(2-thiophenylsulfonyl)-1-piperazinyl)phenyl)-1,1-trifluoro-2-propanol as a white solid (mixture of four isomers, 0.130 g, 37% yield). <sup>1</sup>H NMR (400 MHz, CD<sub>3</sub>OD) δ 7.89 (br d, *J* = 5.1 Hz, 1 H), 7.69–7.63 (m, 1 H), 7.46 (d, *J* = 8.6 Hz, 2 H), 7.40–7.24 (m, 6 H), 6.91 (dd, *J* = 2.0, 9.0 Hz, 2 H), 4.61–4.41 (m, 2 H), 4.26–3.69 (m, 6 H), 3.67–3.38 (m, 3 H), 3.20 (dq, *J* = 3.3, 11.6 Hz, 1 H), 3.07–2.95 (m, 2 H), 2.87–2.68 (m, 1 H), 2.67–2.44 (m, 3 H), 2.38–2.10 (m, 1 H), 1.79–1.58 (m, 4 H).

A 100 mL round-bottomed flask was charged with 2-(4-((2S)-2-((6-(benzyloxy)-3-oxa-8-endo-azabicyclo[3.2.1]oct-8-yl)methyl)-4-(2-thiophenylsulfonyl)-1-piperazinyl)phenyl)-1,1-trifluoro-2-propanol (0.35 g, 0.54 mmol) and 5 mL of CH<sub>2</sub>Cl<sub>2</sub>. After cooling to 0 °C, BCl<sub>3</sub> (1 M in CH<sub>2</sub>Cl<sub>2</sub>, 2.15 mL, 2.15 mmol) was added dropwise. This mixture was allowed to warm to rt and then stirred for an additional 15 min. Then 10 mL of MeOH was added, and the mixture was concentrated onto silica gel and then purified via silica gel chromatography (0–7% MeOH in CH<sub>2</sub>Cl<sub>2</sub>) to give the title compound (0.21 g, 70% yield) as a white solid (mixture of four isomers). <sup>1</sup>H NMR (400 MHz, CD<sub>3</sub>OD) δ 7.92 (d, *J* = 4.9 Hz, 1 H), 7.67 (d, *J* = 3.5 Hz, 1 H), 7.54 (t, *J* = 7.2 Hz, 2 H), 7.28 (t, *J* = 5.3 Hz, 1 H), 7.06 (t, *J* = 9.1 Hz, 2 H), 4.43–4.62 (m, 2H), 3.39–4.24 (m, 13H), 2.66–2.98 (m, 2H), 2.55 (d, *J* = 3.91 Hz, 1H), 1.69 (br s, 3H). *m/z* (ESI, +ve ion) 562.1 (M + H)<sup>+</sup>.

The individual isomers (11–14) were isolated using two sequential chiral SFC purifications. The first separation used a Chiralpak column (21 mm × 250 mm, 5 μm) with 30% MeOH (w/20 mM NH<sub>3</sub>) in supercritical CO<sub>2</sub> at a flow rate of 70 mL/min. The second SFC purification used a Chiralcel OJH column (21 mm × 250 mm, 5 μm) with 25% MeOH (w/20 mM NH<sub>3</sub>) in supercritical CO<sub>2</sub> and a flow rate of 70 mL/min. This sequence produced the four isomers with both diastereomeric and enantiomeric excesses >95%. The absolute

stereochemistries were tentatively assigned based on the X-ray cocrystal structures with hGKRP.

**(1*R*,*5R*,*6R*)-8-(((2*S*)-4-(2-Thiophenylsulfonyl)-1-(4-((1*R*)-2,2,2-trifluoro-1-hydroxy-1-methylethyl)phenyl)-2-piperazinyl)methyl)-3-oxa-8-azabicyclo[3.2.1]octan-6-ol (11).**  $^1\text{H}$  NMR (400 MHz, CD<sub>3</sub>OD)  $\delta$  7.78 (d,  $J$  = 4.9 Hz, 1 H), 7.60–7.45 (m, 1 H), 7.34 (d,  $J$  = 8.8 Hz, 2 H), 7.16 (t,  $J$  = 4.4 Hz, 1 H), 6.80 (s, 2 H), 4.31–4.07 (m, 3 H), 3.92 (d,  $J$  = 11.2 Hz, 2 H), 3.81–3.61 (m, 2 H), 3.52 (s, 2 H), 3.37 (br s, 1 H), 3.10 (d,  $J$  = 3.5 Hz, 1 H), 2.89 (br s, 1 H), 2.79–2.63 (m, 2 H), 2.60–2.15 (m, 4 H), 1.58 (s, 3 H).  $m/z$  (ESI, +ve ion) 562.1 (M + H)<sup>+</sup>.

**(1*R*,*5R*,*6R*)-8-(((2*S*)-4-(2-Thiophenylsulfonyl)-1-(4-((1*S*)-2,2,2-trifluoro-1-hydroxy-1-methylethyl)phenyl)-2-piperazinyl)methyl)-3-oxa-8-azabicyclo[3.2.1]octan-6-ol (12).**  $^1\text{H}$  NMR (400 MHz, CD<sub>3</sub>OD)  $\delta$  7.90 (dd,  $J$  = 1.2, 5.1 Hz, 1 H), 7.66 (d,  $J$  = 2.7 Hz, 1 H), 7.46 (d,  $J$  = 8.8 Hz, 2 H), 7.34–7.21 (m, 1 H), 6.91 (d,  $J$  = 8.8 Hz, 2 H), 4.42–4.27 (m, 1 H), 4.09–3.93 (m, 2 H), 3.88 (d,  $J$  = 10.2 Hz, 1 H), 3.79 (d,  $J$  = 11.3 Hz, 1 H), 3.69–3.56 (m, 2 H), 3.47 (d,  $J$  = 12.7 Hz, 1 H), 3.39–3.35 (m, 1 H), 3.22 (dt,  $J$  = 3.5, 12.1 Hz, 1 H), 3.01 (s, 1 H), 2.89–2.74 (m, 2 H), 2.70–2.48 (m, 4 H), 2.47–2.30 (m, 1 H), 1.69 (s, 3 H).  $m/z$  (ESI, +ve ion) 562.1.

**(1*S*,*5S*,*6S*)-8-(((2*S*)-4-(2-Thiophenylsulfonyl)-1-(4-((1*R*)-2,2,2-trifluoro-1-hydroxy-1-methylethyl)phenyl)-2-piperazinyl)methyl)-3-oxa-8-azabicyclo[3.2.1]octan-6-ol (13).**  $^1\text{H}$  NMR (400 MHz, CD<sub>3</sub>OD)  $\delta$  7.81–7.73 (m, 1 H), 7.58–7.50 (m, 1 H), 7.34 (d,  $J$  = 8.6 Hz, 2 H), 7.19–7.12 (m, 1 H), 6.80 (d,  $J$  = 8.8 Hz, 2 H), 4.35–4.20 (m, 1 H), 3.99 (d,  $J$  = 11.2 Hz, 1 H), 3.84–3.58 (m, 4 H), 3.45 (d,  $J$  = 10.6 Hz, 1 H), 3.42–3.28 (m, 2 H), 3.07 (dt,  $J$  = 3.1, 12.0 Hz, 1 H), 2.83 (d,  $J$  = 6.8 Hz, 1 H), 2.73 (d,  $J$  = 6.1 Hz, 1 H), 2.62 (dd,  $J$  = 9.9, 12.6 Hz, 1 H), 2.57–2.31 (m, 4 H), 2.12 (m, 1 H), 1.57 (s, 3 H).  $m/z$  (ESI, +ve ion) 562.1 (M + H)<sup>+</sup>.

**(1*S*,*5S*,*6S*)-8-(((2*S*)-4-(2-Thiophenylsulfonyl)-1-(4-((1*S*)-2,2,2-trifluoro-1-hydroxy-1-methylethyl)phenyl)-2-piperazinyl)methyl)-3-oxa-8-azabicyclo[3.2.1]octan-6-ol (14).**  $^1\text{H}$  NMR (400 MHz, CD<sub>3</sub>OD)  $\delta$  7.78 (d,  $J$  = 4.9 Hz, 1 H), 7.55 (d,  $J$  = 2.7 Hz, 1 H), 7.36 (d,  $J$  = 8.6 Hz, 2 H), 7.21–7.08 (m, 1 H), 6.82 (d,  $J$  = 8.6 Hz, 2 H), 4.33 (br s, 1 H), 4.01–3.58 (m, 5 H), 3.56–3.43 (m, 1 H), 3.42–3.30 (m, 2 H), 3.16–2.38 (m, 7 H), 2.25–2.03 (m, 1 H), 1.65–1.44 (m, 4 H).  $m/z$  (ESI, +ve ion) 562.1 (M + H)<sup>+</sup>.

**1,1,1,3,3,3-Hexafluoro-2-(4-(4-(phenylsulfonyl)-1-piperazinyl)phenyl)-2-propanol (16).** A 100 mL round-bottomed flask was charged with 1,1,1,3,3,3-hexafluoro-2-(4-(piperazin-1-yl)phenyl)-propan-2-ol<sup>8</sup> (2.19 g, 6.67 mmol), 20 mL of CH<sub>2</sub>Cl<sub>2</sub>, and triethylamine (0.91 g, 1.25 mL, 9.01 mmol). To this was added 2-benzenesulfonyl chloride (1.30 g, 6.67 mmol). After stirring at rt for 2 h, the mixture was diluted with water and extracted with EtOAc. The combined organics extracts were dried (MgSO<sub>4</sub>), filtered, and concentrated to give an oil. This oil was purified by silica gel chromatography (0–50% EtOAc in hexanes) to give 1,1,1,3,3,3-hexafluoro-2-(4-(phenylsulfonyl)-1-piperazinyl)phenyl-2-propanol (1.85 g, 59% yield) as a white solid.  $^1\text{H}$  NMR (400 MHz, CDCl<sub>3</sub>)  $\delta$  = 7.85–7.77 (m, 2 H), 7.67–7.54 (m, 5 H), 7.01–6.92 (m, 2 H), 3.39–3.28 (m, 4 H), 3.27–3.21 (m, 4 H).  $m/z$  (ESI, +ve ion) 469.0 (M + H)<sup>+</sup>.

**2-(4-(4-(5-Amino-2-thiophenyl)sulfonyl)-1-piperazinyl)phenyl)-1,1,1,3,3,3-hexafluoro-2-propanol (17).** A 100 mL round-bottomed flask was charged with 1,1,1,3,3,3-hexafluoro-2-(4-(1-piperazinyl)phenyl)-2-propanol<sup>8</sup> (0.54 g, 1.7 mmol), 10 mL of CH<sub>2</sub>Cl<sub>2</sub>, and 5-bromo-2-thiophenesulfonyl chloride (0.43 g, 1.7 mmol). To this was added triethylamine (0.20 g, 0.28 mL, 2.1 mmol). After 15 min at rt, the mixture was diluted with 10 mL of CH<sub>2</sub>Cl<sub>2</sub> and filtered. The filtrate was concentrated and purified by silica gel chromatography (0–50% EtOAc in hexanes) to give 2-(4-(4-(5-bromo-2-thiophenyl)sulfonyl)-1-piperazinyl)phenyl)-1,1,1,3,3,3-hexafluoro-2-propanol (0.83 g, 91% yield) as a white solid.  $^1\text{H}$  NMR (400 MHz, CD<sub>3</sub>OD)  $\delta$  7.57 (d,  $J$  = 8.8 Hz, 2 H), 7.44 (d,  $J$  = 4.1 Hz, 1 H), 7.31 (d,  $J$  = 3.9 Hz, 1 H), 7.09–6.94 (m, 2 H), 3.39–3.34 (m, 4 H), 3.24–3.18 (m, 4 H).

A 20 mL vial was charged with 2-(4-(4-(5-bromo-2-thiophenyl)sulfonyl)-1-piperazinyl)phenyl)-1,1,1,3,3,3-hexafluoro-2-propanol (0.89 g, 1.61 mmol), 1,1-diphenylmethanimine (0.35 g, 1.93 mmol), sodium *tert*-butoxide (0.37 g, 3.87 mmol), and 6 mL of toluene. To this was added Pd<sub>2</sub>(dba)<sub>3</sub> (0.15 g, 0.16 mmol) and 2,2'-bis-

(diphenylphosphino)-1,1'-binaphthyl (BINAP) (0.25 g, 0.40 mmol). Nitrogen gas was bubbled through the solution for 2 min, and then the vial was sealed and heated at 80 °C for 12 h. The black mixture was then diluted with EtOAc (10 mL) and filtered, and the filtrate was concentrated to give a black tar. Purification via column chromatography on silica gel (0–60% EtOAc in hexanes) provided the intermediate imine. To this was added 5 M HCl (15 mL) and THF (15 mL). After 15 min, 5 M NaOH (15 mL) was added and the mixture was extracted with EtOAc (50 mL). The organics were dried (MgSO<sub>4</sub>), filtered, and concentrated to give an orange foam. Purification via silica gel chromatography (0–70% EtOAc in hexanes) gave an orange oil. Diethylether (25 mL) and hexanes (50 mL) were added, and the resulting white solid was collected by filtration to deliver 2-(4-(4-(5-amino-2-thiophenyl)sulfonyl)-1-piperazinyl)phenyl)-1,1,1,3,3,3-hexafluoro-2-propanol (0.32 g, 40% yield).  $^1\text{H}$  NMR (400 MHz, CD<sub>3</sub>OD)  $\delta$  7.57 (d,  $J$  = 8.8 Hz, 2 H), 7.22 (d,  $J$  = 4.1 Hz, 1 H), 7.03 (d,  $J$  = 9.2 Hz, 2 H), 6.07 (d,  $J$  = 4.1 Hz, 1 H), 3.39–3.26 (m, 4 H), 3.21–3.10 (m, 4 H).  $m/z$  (ESI, +ve ion) 490.0 (M + H)<sup>+</sup>.

**2-(4-(4-(4-Amino-2-thiophenyl)sulfonyl)-1-piperazinyl)phenyl)-1,1,1,3,3,3-hexafluoro-2-propanol (18).** 1,1,1,3,3,3-Hexafluoro-2-(4-(1-piperazinyl)phenyl)-2-propanol dihydrochloride<sup>8</sup> (0.31 g, 0.84 mmol) was dissolved in CH<sub>2</sub>Cl<sub>2</sub> (20 mL) and cooled to 0 °C. To this solution was added triethylamine (0.21 g, 2.10 mmol) followed by 4-nitrothiophene-2-sulfonyl chloride (0.21 g, 0.92 mmol). The reaction was allowed to warm to rt and stirred for 2 h. The mixture was filtered, and the filtrate was concentrated and then purified via reverse-phase preparative HPLC (Phenomenex Gemini C<sub>18</sub> column (150 mm × 30 mm, 10 μm) eluting with 0.1% TFA in CH<sub>3</sub>CN/H<sub>2</sub>O (5–100% over 15 min)) to give 2-(4-(4-(4-nitro-2-thiophenyl)sulfonyl)-1-piperazinyl)phenyl)-1,1,1,3,3,3-hexafluoro-2-propanol (0.086 g, 20%).  $m/z$  (ESI, +ve ion) 520.0 (M + H)<sup>+</sup>.

A 50 mL round-bottomed flask was charged with 2-(4-(4-(4-nitro-2-thiophenyl)sulfonyl)-1-piperazinyl)phenyl)-1,1,1,3,3,3-hexafluoro-2-propanol (0.080 g, 0.154 mmol), ammonium formate (0.049 g, 0.770 mmol), and 10% Pd/C (0.02 g) in EtOH (10 mL). This mixture was stirred under an atmosphere of H<sub>2</sub> (1 atm) for 18 h at rt. The reaction mixture was filtered through a plug of Celite (diatomaceous earth), and the filtrate was concentrated, dissolved in CH<sub>2</sub>Cl<sub>2</sub>, and then filtered for a second time through a small plug of silica gel. The filtrate was concentrated to give 2-(4-(4-(4-amino-2-thiophenyl)sulfonyl)-1-piperazinyl)phenyl)-1,1,1,3,3,3-hexafluoro-2-propanol as an off-white solid (0.023 g, 31% yield).  $^1\text{H}$  NMR (400 MHz, CD<sub>3</sub>OD)  $\delta$  7.58 (d,  $J$  = 8.8 Hz, 2 H), 7.19 (d,  $J$  = 2.0 Hz, 1 H), 7.03 (d,  $J$  = 9.0 Hz, 2 H), 6.60 (d,  $J$  = 1.8 Hz, 1 H), 3.40–3.35 (m, 4 H), 3.23–3.17 (m, 4 H).  $m/z$  (ESI, +ve ion) 490.1 (M + H)<sup>+</sup>.

**2-(4-(4-(2-Aminophenyl)sulfonyl)-1-piperazinyl)phenyl)-1,1,1,3,3,3-hexafluoro-2-propanol (19).** To a 25 mL round-bottomed flask was added 1,1,1,3,3,3-hexafluoro-2-(4-(1-piperazinyl)phenyl)-2-propanol dihydrochloride<sup>8</sup> (0.25 g, 0.62 mmol), triethylamine (0.19 g, 0.26 mL, 1.9 mmol), and CH<sub>2</sub>Cl<sub>2</sub> (6 mL). While stirring at rt, 2-nitrobenzenesulfonyl chloride (0.14 g, 0.62 mmol) was added. The mixture was stirred for 20 min and then concentrated onto silica gel. Purification by silica gel chromatography (0–6% MeOH in CH<sub>2</sub>Cl<sub>2</sub>) afforded 1,1,1,3,3,3-hexafluoro-2-(4-(4-(2-nitrophenyl)sulfonyl)-piperazin-1-yl)phenyl)-2-propanol (0.13 g, 41% yield) as a yellow solid.  $^1\text{H}$  NMR (400 MHz, DMSO-*d*<sub>6</sub>)  $\delta$  8.41 (s, 1 H), 7.97–8.11 (m, 2 H), 7.83–7.97 (m, 2 H), 7.47 (d,  $J$  = 8.6 Hz, 2 H), 7.03 (d,  $J$  = 9.2 Hz, 2 H), 3.31 (br s, 8 H).

To a solution of 1,1,1,3,3,3-hexafluoro-2-(4-(4-(2-nitrophenyl)sulfonyl)piperazin-1-yl)phenyl)-2-propanol (0.13 g, 0.25 mmol) in EtOH (5 mL) was added 10% Pd/C (0.026 g, 0.24 mmol). The reaction was stirred under a hydrogen atmosphere (1 atm) for 4 h at rt. The solution was filtered through Celite (diatomaceous earth), and the filtrate was concentrated onto silica gel. Purification by silica gel chromatography (0–6% MeOH in CH<sub>2</sub>Cl<sub>2</sub>) afforded 2-(4-(4-(2-aminophenyl)sulfonyl)piperazin-1-yl)phenyl)-1,1,1,3,3,3-hexafluoro-2-propanol (0.079 g, 64% yield) as a white solid.  $^1\text{H}$  NMR (400 MHz, DMSO-*d*<sub>6</sub>)  $\delta$  8.40 (s, 1 H), 7.45 (d,  $J$  = 8.8 Hz, 2 H), 7.41 (dd,  $J$  = 1.2, 8.0 Hz, 1 H), 7.28–7.35 (m, 1 H), 7.00 (d,  $J$  = 9.0 Hz, 2 H), 6.87 (d,  $J$  =

8.0 Hz, 1H), 6.66 (t,  $J$  = 7.2 Hz, 1H), 6.09 (s, 2H), 3.22–3.29 (m, 4H), 3.06–3.14 (m, 4H).  $m/z$  (ESI, +ve ion) 483.8 ( $M + H$ )<sup>+</sup>.

**2-(4-(4-(3-Aminophenyl)sulfonyl)-1-piperazinyl)phenyl)-1,1,1,3,3,3-hexafluoro-2-propanol (20).** Following the procedure outlined above for **19**, the reaction of 3-nitrobenzenesulfonyl chloride and 1,1,1,3,3,3-hexafluoro-2-(4-(1-piperazinyl)phenyl)-2-propanol dihydrochloride<sup>8</sup> followed by reduction with 10% Pd/C produced the title compound as a white solid (48% yield over two steps). <sup>1</sup>H NMR (400 MHz, DMSO-*d*<sub>6</sub>)  $\delta$  = 8.39 (s, 1H), 7.46 (d,  $J$  = 8.8 Hz, 2H), 7.25 (t,  $J$  = 7.9 Hz, 1H), 7.09–6.89 (m, 3H), 6.87–6.70 (m, 2H), 5.65 (s, 2H), 3.35–3.26 (m, 4H), 3.05–2.91 (m, 4H).  $m/z$  (ESI, +ve ion) 484.1 ( $M + H$ )<sup>+</sup>.

**2-(4-(4-(4-Aminophenyl)sulfonyl)-1-piperazinyl)phenyl)-1,1,1,3,3,3-hexafluoro-2-propanol (21).** Following the procedure outlined above for **19**, the reaction of 4-nitrobenzenesulfonyl chloride and 1,1,1,3,3,3-hexafluoro-2-(4-(1-piperazinyl)phenyl)-2-propanol dihydrochloride<sup>8</sup> followed by reduction with 10% Pd/C produced the title compound as a white solid (30% yield over two steps). <sup>1</sup>H NMR (400 MHz, CD<sub>3</sub>OD)  $\delta$  7.54 (d,  $J$  = 8.8 Hz, 2H), 7.48 (d,  $J$  = 8.6 Hz, 2H), 6.98 (d,  $J$  = 9.0 Hz, 2H), 6.73 (d,  $J$  = 8.6 Hz, 2H), 3.31–3.26 (m, 4H), 3.11–3.03 (m, 4H).  $m/z$  (ESI, +ve ion) 484.1 ( $M + H$ )<sup>+</sup>.

**2-(4-(4-(2-Amino-4-pyridinyl)sulfonyl)-1-piperazinyl)phenyl)-1,1,1,3,3,3-hexafluoro-2-propanol (22).** A 250 mL round-bottomed flask was charged with 4-bromo-2-chloropyridine (1.00 g, 5.20 mmol) and 20 mL of dry diethylether under a nitrogen atmosphere. The solution was then cooled to -78 °C, where *n*-BuLi (2.5 M in hexanes, 2.08 mL, 5.20 mmol) was added. After stirring for 5 min at -78 °C, sulfur dioxide gas was bubbled through the solution for approximately 1 min. The resulting suspension was allowed to warm to rt and concentrated. To the oily solid was added 20 mL of CH<sub>2</sub>Cl<sub>2</sub> and NCS (0.69 g, 5.20 mmol). After stirring for additional 30 min at rt, 1,1,1,3,3,3-hexafluoro-2-(4-(1-piperazinyl)phenyl)-2-propanol dihydrochloride<sup>8</sup> (2.09 g, 5.20 mmol) and triethylamine (2.10 g, 2.90 mL, 20.8 mmol) were added. After an additional 30 min at rt, 50 mL of water was added and the layers were separated. The organics were dried (MgSO<sub>4</sub>), filtered, concentrated, and purified via silica gel chromatography (0–50% EtOAc in hexanes) to give 2-(4-(4-(2-chloro-4-pyridinyl)sulfonyl)-1-piperazinyl)phenyl)-1,1,1,3,3,3-hexafluoro-2-propanol (1.60 g, 61% yield) as an off-white solid. <sup>1</sup>H NMR (400 MHz, CD<sub>3</sub>OD)  $\delta$  8.68 (d,  $J$  = 5.1 Hz, 1H), 7.82 (s, 1H), 7.72 (dd,  $J$  = 1.4, 5.1 Hz, 1H), 7.56 (d,  $J$  = 8.8 Hz, 2H), 7.00 (d,  $J$  = 9.0 Hz, 2H), 3.36–3.33 (m, 4H), 3.29–3.23 (m, 4H).

A 350 mL pressure vessel was charged with 2-(4-(4-(2-chloro-4-pyridinyl)sulfonyl)-1-piperazinyl)phenyl)-1,1,1,3,3,3-hexafluoro-2-propanol (1.60 g, 3.18 mmol), 15 mL of EtOH, and concentrated ammonium hydroxide (15 mL, 385 mmol). The vessel was sealed, and the mixture was heated at 125 °C for 18 h. After the mixture was allowed to cool to rt, water (50 mL) was added and the organics were extracted with CH<sub>2</sub>Cl<sub>2</sub> (3 × 100 mL). The combined organic extracts were dried (MgSO<sub>4</sub>), filtered, and concentrated. The residue was purified by silica gel chromatography (0–70% EtOAc in hexanes). The resulting solid was washed with CH<sub>2</sub>Cl<sub>2</sub> to give 2-(4-(4-(2-amino-4-pyridinyl)sulfonyl)-1-piperazinyl)phenyl)-1,1,1,3,3,3-hexafluoro-2-propanol (0.10 g, 7% yield) as a white solid. <sup>1</sup>H NMR (400 MHz, CD<sub>3</sub>OD)  $\delta$  = 7.97 (d,  $J$  = 5.5 Hz, 1H), 7.39 (d,  $J$  = 8.6 Hz, 2H), 6.84 (d,  $J$  = 9.2 Hz, 2H), 6.75–6.65 (m, 2H), 3.19–3.12 (m, 4H), 3.08–3.02 (m, 4H).  $m/z$  (ESI, +ve ion) 484.8 ( $M + H$ )<sup>+</sup>.

**2-(4-(6-Amino-3-pyridinyl)sulfonyl)-1-piperazinyl)phenyl)-1,1,1,3,3,3-hexafluoro-2-propanol (23).** A 250 mL round-bottomed flask was charged with 1,1,1,3,3,3-hexafluoro-2-(4-(1-piperazinyl)phenyl)-2-propanol dihydrochloride<sup>8</sup> (2.50 g, 6.23 mmol), 20 mL of CH<sub>2</sub>Cl<sub>2</sub>, triethylamine (2.52 g, 3.47 mL, 24.9 mmol), and 6-chloropyridine-3-sulfonyl chloride<sup>22</sup> (1.32 g, 6.23 mmol). After stirring at rt for 30 min, 150 mL of water was added and the layers were separated. The organics were dried (MgSO<sub>4</sub>), filtered, and concentrated to give an oily solid. To this material was added 10 mL of EtOH and concentrated ammonium hydroxide (9.95 mL, 255 mmol). The vessel was sealed and heated at 120 °C for 12 h. After the mixture was allowed to cool to rt, 100 mL of EtOAc and 50 mL of water were added. The organics were separated, dried (MgSO<sub>4</sub>),

filtered, and concentrated to give an oil. Purification via silica gel chromatography (0–70% EtOAc in hexanes) delivered 2-(4-(6-amino-3-pyridinyl)sulfonyl)-1-piperazinyl)phenyl)-1,1,1,3,3,3-hexafluoro-2-propanol (1.65 g, 55% yield) as an off-white solid. <sup>1</sup>H NMR (400 MHz, CD<sub>3</sub>OD)  $\delta$  8.30 (d,  $J$  = 2.3 Hz, 1H), 7.74 (dd,  $J$  = 2.4, 8.9 Hz, 1H), 7.56 (d,  $J$  = 8.8 Hz, 2H), 7.00 (d,  $J$  = 9.0 Hz, 2H), 6.64 (d,  $J$  = 8.8 Hz, 1H), 3.35–3.30 (m, 4H), 3.17–3.11 (m, 4H).  $m/z$  (ESI, +ve ion) 484.9 ( $M + H$ )<sup>+</sup>.

**2-(4-(2-Amino-5-pyrimidinyl)sulfonyl)-1-piperazinyl)phenyl)-1,1,1,3,3,3-hexafluoro-2-propanol (24).** A 100 mL round-bottomed flask was charged with 1,1,1,3,3,3-hexafluoro-2-(4-(1-piperazinyl)phenyl)-2-propanol dihydrochloride<sup>8</sup> (0.45 g, 1.13 mmol), 10 mL of CH<sub>2</sub>Cl<sub>2</sub>, triethylamine (0.46 g, 0.63 mL, 4.51 mmol), and 2-chloro-5-pyrimidinesulfonyl chloride (0.24 g, 1.13 mmol). After stirring for 15 min at rt, the mixture was concentrated and diluted with 10 mL of EtOH and 10 mL of NH<sub>4</sub>OH. The mixture was stirred at rt for 1 h and then diluted with 50 mL of EtOAc. The organics were separated, dried (MgSO<sub>4</sub>), filtered, and concentrated. The residue was purified by column chromatography on silica gel (0–65% EtOAc in hexanes) to give 2-(4-(2-amino-5-pyrimidinyl)sulfonyl)-1-piperazinyl)phenyl)-1,1,1,3,3,3-hexafluoro-2-propanol (0.22 g, 40% yield). <sup>1</sup>H NMR (400 MHz, CD<sub>3</sub>OD)  $\delta$  8.58 (s, 2H), 7.57 (d,  $J$  = 8.8 Hz, 2H), 7.03 (d,  $J$  = 9.2 Hz, 2H), 3.38–3.34 (m, 4H), 3.22–3.17 (m, 4H).  $m/z$  (ESI, +ve ion) 485.9 ( $M + H$ )<sup>+</sup>.

**2-(4-(6-Amino-3-pyridinyl)sulfonyl)-2-(1-propyn-1-yl)-1-piperazinyl)phenyl)-1,1,1,3,3,3-hexafluoro-2-propanol (25).<sup>9</sup>** A 2 L Erlenmeyer flask was charged with 2-piperazinone (36.5 g, 364 mmol), sodium carbonate (116 g, 1.10 mol), 600 mL of dioxane, and 150 mL of water at room temperature. To this was slowly added benzyl chloroformate (62.1 g, 364 mmol) over 20 min. After the addition was complete, the mixture was stirred for 2 h and then diluted with water and extracted with 2 L of EtOAc. The combined organic extracts were dried (MgSO<sub>4</sub>), filtered, and concentrated to give a white solid. To this solid was added 500 mL of CH<sub>2</sub>Cl<sub>2</sub>, triethylamine (92.6 g, 128 mL, 911 mmol), DMAP (4.45 g, 36.4 mmol), and di-*tert*-butyl dicarbonate (119 g, 546 mmol). After 1 h at room temperature, the mixture was diluted with water and the organics were separated, dried (MgSO<sub>4</sub>), filtered, and concentrated to give a brown oil. To this oil was added 100 mL of CH<sub>2</sub>Cl<sub>2</sub> followed by 1 L of hexane. The resulting white solid was collected by filtration to give 4-benzyl 1-*tert*-butyl 2-oxo-1,4-piperazinedicarboxylate (101 g, 81% yield). <sup>1</sup>H NMR (400 MHz, CDCl<sub>3</sub>)  $\delta$  7.45–7.29 (m, 5H), 5.15 (s, 2H), 4.24 (s, 2H), 3.88–3.74 (m, 2H), 3.74–3.59 (m, 2H), 1.54 (s, 9H).

A 150 mL round-bottomed flask charged with a solution of 4-benzyl 1-*tert*-butyl 2-oxo-1,4-piperazinedicarboxylate (1.41 g, 4.22 mmol) in 5 mL of THF was cooled to 0 °C. 1-Propynylmagnesium bromide (0.5 M in THF, 20.0 mL, 10.0 mmol) was added dropwise over 15 min. The mixture was stirred at 0 °C for 2 h, and then saturated aqueous NH<sub>4</sub>Cl (40 mL) was added. The aqueous phase was extracted with EtOAc (200 mL, then 2 × 100 mL). The organic extracts were dried (Na<sub>2</sub>SO<sub>4</sub>), filtered, and concentrated. The crude product was purified by silica gel chromatography (0–50% EtOAc in hexanes) to afford benzyl (2-((*tert*-butoxycarbonyl)amino)ethyl)(2-oxo-3-pentyn-1-yl)-carbamate (1.55 g, 99% yield) as a clear oil. <sup>1</sup>H NMR (400 MHz, CDCl<sub>3</sub>)  $\delta$  7.39–7.27 (m, 5H), 5.13 (d,  $J$  = 19.4 Hz, 2H), 4.97 (d,  $J$  = 3.9 Hz, 1H), 4.18 (s, 1H), 4.16–4.08 (m, 1H), 3.44 (td,  $J$  = 5.8, 11.7 Hz, 2H), 3.32–3.16 (m, 2H), 2.00 (d,  $J$  = 13.3 Hz, 3H), 1.42 (d,  $J$  = 4.7 Hz, 9H).

A 3 L round-bottomed flask was charged with 2-((*tert*-butoxycarbonyl)amino)ethyl)(2-oxo-3-pentyn-1-yl)carbamate (82.2 g, 219 mmol) and 300 mL of CH<sub>2</sub>Cl<sub>2</sub>. After cooling to -10 °C, TFA (169 mL, 2.20 mol) was added, and the resulting dark solution was stirred at room temperature for 15 min. Sodium triacetoxyborohydride (186 g, 878 mmol) was added portionwise over 10 min. After 2 h, the mixture was concentrated, diluted with EtOAc (1 L), and neutralized with 5 N NaOH. The layers were separated, and the organic extracts were washed with brine, dried (MgSO<sub>4</sub>), filtered, and concentrated. The resulting orange oil was purified via silica gel chromatography (0–4.5% MeOH in CH<sub>2</sub>Cl<sub>2</sub>) to give benzyl 3-(1-propyn-1-yl)-1-piperazinecarboxylate (43.7 g, 77% yield) as a brown foam. <sup>1</sup>H

NMR (400 MHz, CDCl<sub>3</sub>) δ 7.43–7.30 (m, 5 H), 5.28–5.04 (m, 2 H), 4.05–3.61 (m, 5 H), 3.37 (br s, 1 H), 3.03 (br s, 1 H), 1.79 (br s, 3 H) (one exchangeable proton was not observed).

A 150 mL reaction vessel was charged with benzyl 3-(prop-1-yn-1-yl)piperazine-1-carboxylate (2.88 g, 11.2 mmol), 2-(4-bromophenyl)-1,1,1,3,3,3-hexafluoro-2-propanol<sup>3</sup> (4.36 g, 13.5 mmol), dicyclohexyl-(2',6'-diisopropoxy-[1,1'-biphenyl]-2-yl)phosphine (RuPhos) (0.530 g, 1.14 mmol), chloro(2-dicyclohexylphosphino-2',6'-di-i-propoxy-1,1'-biphenyl)[2-(2-aminoethyl)phenyl]palladium(II), methyl *tert*-butylether adduct (RuPhos first generation precatalyst) (0.417 g, 0.572 mmol), sodium *tert*-butoxide (2.73 g, 28.4 mmol), and toluene (35 mL). Argon was bubbled through the solution for 10 min. The vessel was sealed and heated at 100 °C for 1.5 h. After the reaction was allowed to cool to room temperature, water (100 mL) was added. The aqueous phase was extracted with EtOAc (3 × 100 mL), and the combined organic extracts were washed with brine, dried (Na<sub>2</sub>SO<sub>4</sub>), filtered, and concentrated. The crude product was purified by silica gel chromatography (0–50% EtOAc in hexanes) to afford benzyl 3-(1-propyn-1-yl)-4-(4-(2,2,2-trifluoro-1-hydroxy-1-(trifluoromethyl)ethyl)phenyl)-1-piperazinecarboxylate (3.84 g, 69% yield) as a yellow solid. <sup>1</sup>H NMR (400 MHz, CDCl<sub>3</sub>) δ 7.59 (d, J = 8.6 Hz, 2 H), 7.44–7.29 (m, 5 H), 6.99 (d, J = 9.0 Hz, 2 H), 5.32–5.08 (m, 2 H), 4.48–4.17 (m, 3 H), 3.50–3.02 (m, 5 H), 1.69 (br s, 3 H).

A 500 mL round-bottomed flask was charged with benzyl 3-(1-propyn-1-yl)-4-(4-(2,2,2-trifluoro-1-hydroxy-1-(trifluoromethyl)ethyl)phenyl)-1-piperazinecarboxylate (3.13 g, 6.25 mmol) and TFA (40 mL). Trifluoromethanesulfonic acid (TfOH) (1.25 mL, 14.1 mmol) was added dropwise at room temperature. After 5 min, additional TfOH (0.45 mL, 5.1 mmol) was added. After an additional 10 min, solid NaHCO<sub>3</sub> was carefully added in portions until effervescence ceased. Saturated aqueous NaHCO<sub>3</sub> (250 mL) was then added slowly to bring the pH to approximately 7. The aqueous phase was then extracted with EtOAc (100 mL). The organic layers were combined and washed with water (200 mL) and brine (200 mL) then dried (Na<sub>2</sub>SO<sub>4</sub>), filtered, and concentrated to afford a tan solid. To this solid was added CH<sub>2</sub>Cl<sub>2</sub> (30 mL) and triethylamine (3.63 g, 5.00 mL, 35.9 mmol). 6-Chloropyridine-3-sulfonyl chloride<sup>22</sup> (1.58 g, 7.43 mmol) was then added in portions at 0 °C. The brown mixture was stirred at 0 °C for 10 min, and then the reaction mixture was concentrated and purified by silica gel chromatography (twice, 0–50% EtOAc in hexanes) to afford 2-(4-(6-chloro-3-pyridinyl)sulfonyl)-2-(1-propyn-1-yl)-1-piperazinylphenyl)-1,1,1,3,3,3-hexafluoro-2-propanol (3.46 g, 100% yield) as an off-white solid. <sup>1</sup>H NMR (400 MHz, CDCl<sub>3</sub>) δ 8.84 (d, J = 2.2 Hz, 1 H), 8.06 (dd, J = 2.3, 8.4 Hz, 1 H), 7.60 (d, J = 8.6 Hz, 2 H), 7.52 (d, J = 8.4 Hz, 1 H), 7.01–6.93 (m, 2 H), 4.46 (br s, 1 H), 3.85 (t, J = 11.2 Hz, 2 H), 3.52–3.33 (m, 3 H), 2.95 (dd, J = 3.1, 11.3 Hz, 1 H), 2.81 (dt, J = 3.7, 11.3 Hz, 1 H), 1.78 (d, J = 1.6 Hz, 3 H).

A 20 mL sealed tube was charged with 2-(4-(6-chloro-3-pyridinyl)sulfonyl)-2-(1-propyn-1-yl)-1-piperazinylphenyl)-1,1,1,3,3,3-hexafluoro-2-propanol (0.340 g, 0.627 mmol), concentrated ammonium hydroxide (5.00 mL, 38.5 mmol), and EtOH (5 mL). The reaction mixture was heated in a microwave reactor at 120 °C for 1 h. The reaction mixture was then heated in a heating block at 110 °C for 5 h and then was concentrated and purified by silica gel chromatography (25 g of silica, 30–80% EtOAc in hexanes) to afford 2-(4-(6-amino-3-pyridinyl)sulfonyl)-2-(1-propyn-1-yl)-1-piperazinylphenyl)-1,1,1,3,3,3-hexafluoro-2-propanol (0.289 g, 88% yield) as a off-white solid. <sup>1</sup>H NMR (400 MHz, CDCl<sub>3</sub>) δ 8.49 (br s, 1 H), 7.80 (dd, J = 2.3, 8.8 Hz, 1 H), 7.59 (d, J = 8.8 Hz, 2 H), 6.97 (d, J = 9.0 Hz, 2 H), 6.55 (d, J = 8.8 Hz, 1 H), 5.05 (s, 2 H), 4.46 (br s, 1 H), 3.85–3.72 (m, 2 H), 3.54 (br s, 1 H), 3.50–3.34 (m, 2 H), 2.83 (dd, J = 3.3, 11.0 Hz, 1 H), 2.69 (dt, J = 3.4, 11.0 Hz, 1 H), 1.80 (s, 3 H). *m/z* (ESI, +ve ion) 523.1 (M + H)<sup>+</sup>.

The individual enantiomers (**26** and **27**) were isolated using chiral SFC (Chiralpak ADH column (21 mm × 250 mm, 5 μm) eluting with 35% MeOH in supercritical CO<sub>2</sub> (total flow was 70 mL/min)). This produced the two isomers with enantiomeric excesses of >98%. The absolute stereochemistries of **26** (second eluting peak) and **27** (first

eluting peak) were assigned based on the cocrystal structure with hGKRP.

*2-(4-((2*R*)-4-((6-Amino-3-pyridinyl)sulfonyl)-2-(1-propyn-1-yl)-1-piperazinyl)phenyl)-1,1,1,3,3,3-hexafluoro-2-propanol* (**26**). <sup>1</sup>H NMR (400 MHz, CDCl<sub>3</sub>) δ 8.49 (d, J = 1.8 Hz, 1 H), 7.78 (dd, J = 2.3, 8.8 Hz, 1 H), 7.59 (d, J = 8.6 Hz, 2 H), 6.97 (d, J = 9.0 Hz, 2 H), 6.54 (d, J = 8.8 Hz, 1 H), 4.97 (s, 2 H), 4.46 (br s, 1 H), 3.77 (t, J = 11.7 Hz, 2 H), 3.67 (br s, 1 H), 3.51–3.33 (m, 2 H), 2.82 (dd, J = 3.3, 11.0 Hz, 1 H), 2.68 (dt, J = 3.9, 11.1 Hz, 1 H), 1.79 (d, J = 2.0 Hz, 3 H). *m/z* (ESI, +ve ion) 523.2 (M + H)<sup>+</sup>.

*2-(4-((2*S*)-4-((6-Amino-3-pyridinyl)sulfonyl)-2-(1-propyn-1-yl)-1-piperazinyl)phenyl)-1,1,1,3,3,3-hexafluoro-2-propanol* (**27**). <sup>1</sup>H NMR (400 MHz, CDCl<sub>3</sub>) δ 8.48 (d, J = 2.3 Hz, 1 H), 7.77 (dd, J = 2.5, 8.8 Hz, 1 H), 7.57 (d, J = 8.8 Hz, 2 H), 6.95 (d, J = 9.2 Hz, 2 H), 6.52 (d, J = 8.8 Hz, 1 H), 4.94 (s, 2 H), 4.44 (br s, 1 H), 3.82–3.71 (m, 2 H), 3.58–3.33 (m, 3 H), 2.81 (dd, J = 3.2, 11.1 Hz, 1 H), 2.67 (dt, J = 3.9, 11.0 Hz, 1 H), 1.78 (d, J = 2.2 Hz, 3 H). *m/z* (ESI, +ve ion) 523.2 (M + H)<sup>+</sup>.

*(2S)-2-(4-((2*S*)-4-((6-Amino-3-pyridinyl)sulfonyl)-2-(1-propyn-1-yl)-1-piperazinyl)phenyl)-1,1,1-trifluoro-2-propanol* (**28**). Compound **28** was synthesized according to the procedure described for the synthesis of **25** using (S)-2-(4-bromophenyl)-1,1,1-trifluoro-2-propanol<sup>8</sup> in place of 2-(4-bromophenyl)-1,1,1,3,3,3-hexafluoropropan-2-ol. The individual isomers were isolated using preparative SFC (Chiralpak AD-H column (4.6 mm × 150 mm, 5 μm) eluting with 60% supercritical CO<sub>2</sub> in 40% MeOH with 40 mM ammonia at a flow rate of 60 mL/min) to give the title compound (first eluting peak) in >99% diastereomeric excess. <sup>1</sup>H NMR (300 MHz, CDCl<sub>3</sub>) δ 8.50 (s, 1 H), 7.83–7.74 (m, 1 H), 7.47 (d, J = 8.6 Hz, 2 H), 6.94 (d, J = 8.8 Hz, 2 H), 6.54 (d, J = 8.6 Hz, 1 H), 5.01 (s, 2 H), 4.42 (br s, 1 H), 3.74 (t, J = 10.2 Hz, 2 H), 3.44–3.31 (m, 2 H), 2.86 (dd, J = 3.1, 11.2 Hz, 1 H), 2.78–2.60 (m, 1 H), 2.38 (br s, 1 H), 1.79 (d, J = 1.9 Hz, 3 H), 1.76 (s, 3 H). *m/z* (ESI, +ve ion) 469.2 (M + H)<sup>+</sup>.

*(2*R*)-2-(4-((2*S*)-4-((6-Amino-3-pyridinyl)sulfonyl)-2-(1-propyn-1-yl)-1-piperazinyl)phenyl)-1,1,1-trifluoro-2-propanol* (**29**). Compound **29** was synthesized according to the procedure described for **25** using (R)-2-(4-bromophenyl)-1,1,1-trifluoro-2-propanol<sup>8</sup> in place of 2-(4-bromophenyl)-1,1,1,3,3,3-hexafluoropropan-2-ol. The individual isomers were isolated using preparative SFC (Chiralpak AD-H column (21 mm × 150 mm, 5 μm) eluting with 50% liquid CO<sub>2</sub> in 50% MeOH with 20 mM ammonia at a flow rate of 70 mL/min) to give the title compound (first eluting peak) with >99% diastereomeric excess. <sup>1</sup>H NMR (300 MHz, CDCl<sub>3</sub>) δ 8.49 (s, 1 H), 7.78 (dd, J = 2.3, 8.8 Hz, 1 H), 7.46 (d, J = 8.6 Hz, 2 H), 7.00–6.87 (m, 2 H), 6.60–6.47 (m, 1 H), 4.99 (s, 2 H), 4.41 (d, J = 2.3 Hz, 1 H), 3.82–3.65 (m, 2 H), 3.37 (dd, J = 2.8, 7.3 Hz, 2 H), 2.85 (dd, J = 3.4, 11.1 Hz, 1 H), 2.70 (td, J = 7.3, 11.4 Hz, 1 H), 2.39 (s, 1 H), 1.77 (d, J = 2.0 Hz, 3 H), 1.75 (d, J = 0.7 Hz, 3 H). *m/z* (ESI, +ve ion) 469.0 (M + H)<sup>+</sup>.

*2-(4-((2*R*)-4-((6-Amino-3-pyridinyl)sulfonyl)-2-(1-propyn-1-yl)-1-piperazinyl)phenyl)-1,1,1,3,3,3-hexafluoro-2-propanol* (**30**). Following the procedure described above for **25**, chloro(1-butyn-1-yl)magnesium (generated from 1-butyne and *i*-PrMgCl) produced the title compound as a mixture of enantiomers. <sup>1</sup>H NMR (400 MHz, CD<sub>3</sub>OD) δ 8.31 (d, J = 2.3 Hz, 1 H), 7.74 (dd, J = 2.4, 8.9 Hz, 1 H), 7.57 (d, J = 8.8 Hz, 2 H), 7.04 (d, J = 9.2 Hz, 2 H), 6.63 (d, J = 8.4 Hz, 1 H), 4.76–4.57 (m, 1 H), 3.82–3.68 (m, 2 H), 3.57–3.44 (m, 1 H), 3.29–3.20 (m, 1 H), 2.85–2.73 (m, 1 H), 2.68–2.45 (m, 1 H), 2.14 (dd, J = 1.9, 7.5 Hz, 2 H), 1.04 (t, J = 7.5 Hz, 3 H). *m/z* (ESI, +ve ion) 537.2 (M + H)<sup>+</sup>.

*2-(4-((2*S*)-4-((6-Amino-3-pyridinyl)sulfonyl)-2-(cyclopropylethynyl)-1-piperazinyl)phenyl)-1,1,1,3,3,3-hexafluoro-2-propanol* (**31**). Following the procedure described above for **25**, chloro(cyclopropylethynyl)magnesium (generated from ethynylcyclopropane and *i*-PrMgCl) produced the title compound as a mixture of enantiomers. <sup>1</sup>H NMR (400 MHz, DMSO-*d*<sub>6</sub>) δ 8.45 (s, 1 H), 8.23 (br s, 1 H), 7.63 (d, J = 9.0 Hz, 1 H), 7.26 (d, J = 8.6 Hz, 1 H), 7.07–6.94 (m, 3 H), 6.53 (d, J = 8.8 Hz, 1 H), 5.46 (br s, 1 H), 4.42 (br s, 1 H), 4.29 (br s, 1 H), 3.56 (br s, 1 H), 3.46–3.34 (m, 1 H), 3.24 (br s, 2 H), 2.94 (d, J = 10.8 Hz, 2 H), 2.84–2.69 (m, 1 H), 2.71–2.52 (m, 3 H), 2.06 (br s, 1 H). *m/z* (ESI, +ve ion) 549.2 (M + H)<sup>+</sup>.

**2-(4-(4-((6-Amino-3-pyridinyl)sulfonyl)-2-(3,3-dimethyl-1-butyn-1-yl)-1-piperazinyl)phenyl)-1,1,3,3-hexafluoro-2-propanol (32).** Following the procedure described above for **25**, chloro(3,3-dimethyl-1-butyn-1-yl)magnesium (generated from 3,3-dimethyl-1-butyn-1-yl) and *i*-PrMgCl produced the title compound as a mixture of enantiomers. <sup>1</sup>H NMR (400 MHz, CD<sub>3</sub>OD) δ 8.32 (d, *J* = 2.0 Hz, 1 H), 7.74 (dd, *J* = 2.4, 8.9 Hz, 1 H), 7.58 (d, *J* = 8.8 Hz, 2 H), 7.05 (d, *J* = 9.0 Hz, 2 H), 6.63 (d, *J* = 9.0 Hz, 1 H), 4.68–4.58 (m, 1 H), 3.70 (d, *J* = 11.2 Hz, 2 H), 3.46 (d, *J* = 12.1 Hz, 1 H), 3.28–3.22 (m, 1 H), 2.80 (dd, *J* = 3.3, 11.3 Hz, 1 H), 2.70–2.50 (m, 1 H), 1.11 (s, 9 H). *m/z* (ESI, +ve ion) 565.1 (M + H)<sup>+</sup>.

## ■ ASSOCIATED CONTENT

### Supporting Information

Standard deviations for the *in vitro* activities listed in Tables 1–3, *rat in vivo* PK data for analogues **11–14**, and hGK SPR data for **27**, **29**, and **33**. This material is available free of charge via the Internet at <http://pubs.acs.org>.

### Accession Codes

PDB ID codes for **1**, **23**, and **27** bound to hGKRP are 4LY9, 4MRO, and 4MQU, respectively.

## ■ AUTHOR INFORMATION

### Corresponding Author

\*Phone: 805-313-5153. E-mail: david01@amgen.com.

### Present Address

▽ For J.Z.: JD Consulting, 1969 Roadrunner Avenue, Thousand Oaks, California 91360, United States.

### Notes

The authors declare the following competing financial interest(s): The authors declare competing financial interests as employees of Amgen Inc.

## ■ ACKNOWLEDGMENTS

We acknowledge Kyung Gahm, Wesley Barnhart, and Samuel Thomas for conducting the SFC separations, Robert Kurzeja for providing the purified proteins, and Robert Wahl and Kathy Chen for assay development. Additionally, we thank Scott Simonet, Murielle Véniant, Dean Hickman, Philip Tagari, and Randall Hungate for their support of this research.

## ■ ABBREVIATIONS USED

GK, glucokinase; GKA, glucokinase activator; GKRP, glucokinase regulatory protein; *S*<sub>0.5</sub>, concentration at which the enzyme is 50% active; *V*<sub>max</sub>, maximum velocity; RLM, rat liver microsomes; HLM, human liver microsomes; CL, clearance; MRT, mean resonance time; PPB, plasma protein binding; *f*<sub>u</sub>, fraction unbound; IHC, immunohistochemistry; DMEM, Dulbecco's Modified Eagle Medium; AAALAC, Association for Assessment and Accreditation of Laboratory Animal Care

## ■ REFERENCES

- (1) Matschinsky, F. M. GKAs for Diabetes Therapy: Why No Clinically Useful Drug after Two Decades of Trying? *Trends Pharmacol. Sci.* **2013**, *34*, 90–99.
- (2) Baltrusch, S.; Tiedge, M. Glucokinase Regulatory Network in Pancreatic  $\beta$ -Cells and Liver. *Diabetes* **2006**, *55* (Suppl 2), 55–64.
- (3) Sarabu, R.; Grimsby, J. Targeting Glucokinase Activation for the Treatment of Type 2 Diabetes—A Status Review. *Curr. Opin. Drug Discovery Dev.* **2005**, *8*, 631–637.
- (4) Coghlan, M.; Leighton, B. Glucokinase Activators in Diabetes Management. *Expert Opin. Invest. Drugs* **2008**, *17*, 145–167.

(5) Rees, M. G.; Gloyn, A. L. Small Molecular Glucokinase Activators: Has Another New Anti-Diabetic Therapeutic Lost Favour? *Br. J. Pharmacol.* **2013**, *168* (2), 335–338.

(6) Pfefferkorn, J. A. Strategies For the Design of Hepatoselective Glucokinase Activators to Treat Type 2 Diabetes. *Expert Opin. Drug Discovery* **2013**, *8*, 319–330.

(7) Matschinsky, F. M.; Van der Kooi, J. M.; Zelent, B.; Naji, A.; Doliba, N.; Sarabu, R.; Li, C.; Grimsby, J. Glucokinase Activators for Diabetes Therapy. *Diabetes Care* **2011**, *34* (Suppl 2), S236–S243.

(8) Ashton, K. S.; Andrews, K. L.; Bryan, M. C.; Chen, J.; Chen, K.; Chen, M.; Chmait, S.; Croghan, M.; Cupples, R.; Fotsch, C.; Helmering, J.; Jordan, S. R.; Kurzeja, R. J. M.; Michelsen, K.; Pennington, L. D.; Poon, S. F.; Sivits, G.; Van, G.; Vonderfecht, S. L.; Wahl, R. C.; Zhang, J.; Lloyd, D. J.; Hale, C.; St. Jean, D. J., Jr. Small Molecule Disruptors of the Glucokinase–Glucokinase Regulatory Protein Interaction: 1. Discovery of a Novel Tool Compound for In Vivo Proof-of-Concept. *J. Med. Chem.* **2014**, DOI jm4016735.

(9) Lloyd, D. J.; St. Jean, D. J., Jr.; Kurzeja, R. J. M.; Wahl, R. C.; Michelsen, K.; Cupples, R.; Chen, M.; Wu, J.; Sivits, G.; Helmering, J.; Ashton, K. S.; Pennington, L. D.; Fotsch, C. H.; Vazir, M.; Chen, K.; Chmait, S.; Zhang, J.; Liu, L.; Norman, M. H.; Andrews, K. A.; Bartberger, M. D.; Van, G.; Galbreath, E. J.; Vonderfecht, S. L.; Wang, M.; Jordan, S. R.; Véniant, M. M.; Hale, C. Anti-Diabetic Effects of a Glucokinase Regulatory Protein Small Molecule Disruptor. *Nature* **2013**, *504*, 437–440.

(10) The average unbound drug concentration at *C*<sub>max</sub> was 0.032  $\mu$ M. The EC<sub>50</sub> value for **1** in mouse hepatocytes was 1.79  $\mu$ M.

(11) Ashton, K.; Bartberger, M. D.; Bo, Y.; Bryan, M. C.; Croghan, M.; Fotsch, C. H.; Hale, C. H.; Kunz, R. K.; Liu, L.; Nishimura, N.; Norman, M. H.; Pennington, L. D.; Poon, S. F.; Stec, M. M.; St. Jean, D. J., Jr.; Tamayo, N. A.; Tegley, C. M.; Yang, K. Preparation of sulfonylpiperazine derivatives that interact with glucokinase regulatory protein for the treatment of diabetes and other diseases. PCT Int. Appl. WO 2012027261, 2012.

(12) Wolff, M.; Kauschke, S. G.; Schmidt, S.; Heilker, R. Activation and Translocation of Glucokinase in Rat Primary Hepatocytes Monitored by High Content Image Analysis. *J. Biomol. Screening* **2008**, *13*, 837–846.

(13) Because of the greater accessibility of rat liver microsomes, RLM data was used as a surrogate for *in vitro* mouse metabolism. We observed a strong correlation between the two species (data not shown).

(14) Chen, Z.; Venkatesan, A. M.; Dos Santos, O.; Delos Santos, E.; Dehnhardt, C. M.; Ayral-Kaloustian, S.; Ashcroft, J.; McDonald, L. A.; Mansour, T. S. Stereoselective Synthesis of an Active Metabolite of the Potent PI3 Kinase Inhibitor PKI-179. *J. Org. Chem.* **2010**, *75*, 1643–1651.

(15) See Supporting Information.

(16) Gleeson, M. P. Generation of a Set of Simple, Interpretable ADMET Rules of Thumb. *J. Med. Chem.* **2008**, *51*, 817–834.

(17) Gleeson, M. P.; Bravi, G.; Modi, S.; Lowe, D. ADMET Rules of Thumb II: A Comparison of the Effects of Common Substituents on a Range of ADMET Parameters. *Bioorg. Med. Chem.* **2009**, *17*, 5906–5919.

(18) St. Jean, D. J., Jr.; Fotsch, C. Mitigating Heterocycle Metabolism in Drug Discovery. *J. Med. Chem.* **2012**, *55*, 6002–6020.

(19) Indeed, an NH-engaging water molecule is observed in other *in-house* cocrystal structures not possessing an occluding substituent in this region.

(20) B3LYP/6-31G\* optimizations of methyl- and propynyl substituted, S-phenyl-N-phenylpiperazine sulfonamides give rise to an axial–equatorial energy difference of ca. 0.9 and 1.3 kcal/mol, respectively, suggesting *a* > 75% population of the axial conformer. Additional CPCM single-point energy calculations in an aqueous solvent model (UAKS radii; B3LYP/6-31G\*; Gaussian 03, revision D.01) further support the preference for the axial substituent orientation (ca. 1.2 and 1.1 kcal/mol, respectively) regardless of the polarity of the medium.

- (21) Biscoe, M. R.; Fors, B. P.; Buchwald, S. L. A New Class of Easily Activated Palladium Precatalysts for Facile C–N Cross-Coupling Reactions and the Low Temperature Oxidative Addition of Aryl Chlorides. *J. Am. Chem. Soc.* **2008**, *130*, 6686–6687.
- (22) Hogan, P. J.; Cox, B. G. Aqueous Process Chemistry: The Preparation of Aryl Sulfonyl Chlorides. *Org. Process Res. Dev.* **2009**, *13*, 875–879.
- (23) Kobayashi, K.; Forte, T. M.; Taniguchi, S.; Ishida, B. Y.; Oka, K.; Chan, L. The *db/db* Mouse, A Model for Diabetic Dyslipidemia: Molecular Characterization and Effects of Western Diet Feeding. *Metabolism*. **2000**, *49*, 22–31.
- (24) Although this was not predicted based on the mouse PK profiles (C57Bl6), the unbound exposure of **27** was significantly higher in *db/db* mice when compared to **29** (approximately 6  $\mu$ M for **27** vs 0.8  $\mu$ M for **29**). This likely contributed to the more robust efficacy observed with **27**.
- (25) No PD data was collected from the animals treated with **29**. The unbound concentrations of **29** were 0.058, 0.240, and 0.786  $\mu$ M for the 10, 30, and 100 mg/kg dose, respectively.
- (26) Grimsby, J.; Sarabu, R.; Corbett, W. L.; Haynes, N.-E.; Bizzarro, F. T.; Coffey, J. W.; Guertin, K. R.; Hilliard, D. W.; Kester, R. F.; Mahaney, P. E.; Marcus, L.; Qi, L.; Spence, C. L.; Tengi, J.; Mafnuson, M. A.; Chu, C. A.; Dvorozniak, M. T.; Matschinsky, F. M.; Grippo, J. F. Allosteric Activators of Glucokinase: Potential Role in Diabetes Therapy. *Science* **2003**, *301*, 370–373.
- (27) It should be noted that *db/db* mice are susceptible to fluctuations in blood glucose values as a function of time of day and handling. This was reflected in the differences in vehicle blood glucose levels at 4 and 8 h.
- (28) SPR data for **27**, **29**, and **33** are supplied in the Supporting Information.
- (29) Kreamer, B. L.; Staecker, J. L.; Sawada, N.; Sattler, G. L.; Hsia, M. T. S.; Pitot, H. C. Use of a Low-Speed, Iso-Density Percoll Centrifugation Method to Increase the Viability of Isolated Rat Hepatocyte Preparations. *In Vitro Cell Dev. Biol.* **1986**, *22*, 201–211.
- (30) Gallego, M. T.; Brunet, E.; Ruano, J. L. G. Conformational Analysis of Methylthiazanes: The Problem of the Me–C–N–Me Gauche Interaction. *J. Org. Chem.* **1993**, *58*, 3905–3911.
- (31) Frenette, R.; Blouin, M.; Brideau, C.; Chauret, N.; Ducharme, Y.; Friesen, R. W.; Hamel, P.; Jones, T. R.; Laliberté, F.; Li, C.; Masson, P.; McAuliffe, M.; Girard, Y. Substituted 4-(2,2-Diphenylethyl)pyridine-N-oxides as Phosphodiesterase-4 Inhibitors: SAR Study Directed Toward the Improvement of Pharmacokinetic Parameters. *Bioorg. Med. Chem. Lett.* **2002**, *12*, 3009–3013.